ROSTANGA PULCHRA: ONE SPECIES OR THREE, DIFFERENTIATING MORPHOLOGY WITHIN A CRYPTIC SPECIES COMPLEX

by

WILLIAM R. BIRD

A THESIS

Presented to the Department of Biology
and the Robert D. Clark Honors College
in partial fulfillment of the requirements for the degree of
Bachelor of Science

March 2026

An Abstract of the Thesis of

William Bird for the degree of Bachelor of Science
in the Department of Biology to be taken March 2026

Title: *Rostanga pulchra:* One Species or Three, Differentiating Morphology Within a Cryptic Species Complex

Approved: *Richard B. Emlet, Ph.D*
Primary Thesis Advisor

The nudibranch *Rostanga pulchra*, first described by F.M. MacFarland in 1905, has long been regarded as a single, morphologically variable species distributed along the Pacific coast of North America. Recent DNA barcoding, however, reveals that *R. pulchra* represents a cryptic species complex comprising at least three genetically distinct operational taxonomic units (OTUs, a term which is commonly used when species are being identified by DNA barcoding alone) occurring sympatrically in Oregon. Delineating species, whether cryptic or not, is fundamental to biology as it underpins accurate biodiversity estimation, ecological interpretation, and evolutionary inference.

This thesis integrates DNA barcoding with comprehensive morphological analyses to identify diagnostic characteristics that distinguish the three genetically distinct groups, in a revival of the golden age of biological observation. While molecular tools are powerful for detecting hidden diversity, the ability to differentiate species morphologically is equally essential for practical identification, ecological study, and formal taxonomic description. Live external morphological surveys revealed differences in the structure of dorsal caryophyllidia —

specifically relative spicule height and spicule position—as well as in minute spot aggregation and density. Radular morphology, examined using scanning electron microscopy (SEM), revealed two useful diagnostic features: the angle of the inner pleural tooth base and length of the inner pleural tooth basal marginal facing extension. Egg diameter was also measured and evaluated as a potential species-level character.

Together, dorsal caryophyllidium microstructure, minute spot aggregation patterns, radular metrics, and egg diameter provide a cohesive morphological framework for distinguishing members of the *Rostanga pulchra* species complex and form the foundation for future species descriptions. Moreover, with newly identified characteristics of each OTU, a hypothesis of the true identity of *Rostanga pulchra* is made. More broadly, the framework presented here offers a methodological template for resolving additional cryptic species complexes within Discodorididae and other nudibranchs.

Acknowledgments

I extend my deepest gratitude to Dr. Richard Emlet for his unwavering guidance, expertise, and remarkable patience throughout a project that seemed, at times, governed by Murphy's Law. His steadfast commitment to rigorous and accurate science challenged me daily and pushed this work to a level it would not otherwise have reached. More importantly, his mentorship shaped not only this project, but also my identity as a researcher, helping me discover a lasting passion for scientific inquiry.

I am sincerely grateful to Dr. Jesse Wilson for his consistent support and generosity with his time; he was always willing to meet, discuss ideas, and offer thoughtful insight. His mentorship fostered both independence and confidence, empowering me to take ownership of this project and see it through to completion.

I also wish to thank my classmates and friends who provided support in specimen collection, revisional help, and morale: Tea Bland, Claire Mullin, Naya Meuller, Mark Leahey, Nate Hart, Maya Selesnick, and Jade Peairson. I am also grateful to Nicholas Bird for his continued assistance in statistical methodology.

I'd also like to express gratitude for the exceptional faculty of the Oregon Institute of Marine Biology, whose teaching formed the foundation of my scientific training. Extended thanks to Dr. George von Dassow for sharing his expertise in scanning electron microscopy, Dr. Rowan McLachlan for her guidance in statistical analysis, and Dr. Svetlana Maslakova for her instruction in PCR techniques.

Finally, I offer my deepest thanks to my parents for their unwavering support throughout my education and during the completion of this thesis. Their encouragement made this achievement possible.

Table of Contents

List of Figures

List of Tables

Introduction

Cryptic species complexes—defined as multiple genetically distinct species that are morphologically indistinguishable—are common throughout the tree of life, particularly in marine taxa (Bickford et al. 2006). In such systems, biodiversity remains hidden beneath superficial similarity, obscuring true species richness and complicating ecological, evolutionary, and conservation-based interpretations.

The nudibranch *Rostanga pulchra*, a small orange dorid common along the west coast of North America, has long been regarded as a single morphologically variable species. However, unpublished molecular work conducted by Richard Emlet, Yvonne Moreira-Andrade, and Sof Fox revealed the presence of three genetically distinct operational taxonomic units (OTUs, a term used when species are being identified by DNA barcoding) occurring sympatrically in Oregon. In this thesis, OTU1, OTU2, and OTU3 refer to the three distinct clades identified within this complex. These previous studies also preliminarily examined divergence in OTU diet and egg diameter. However, without a concrete morphological method to distinguish clades, research remained dependent on molecular barcoding to assign traits to OTUs. Without a practical framework for differentiating OTUs, rapid preliminary assessments and accurate evaluation of sample sizes were impossible.

The primary aim of this thesis was to develop a repeatable morphological framework capable of diagnosing these three OTUs, providing a foundation for future research, species descriptions, and additional cryptic species complexes within Discodorididae. Moreover, these morphological traits allow comparison with the original species description and support a hypothesis concerning which lineage represents the nominal species *Rostanga pulchra*. First, this introduction seeks to review features of dorid morphology relevant to cryptic species complexes,

synthesize existing research on *Rostanga pulchra,* and extend the relevance of resolving cryptic species complexes.

.

Morphology and Past Cryptic Species Complexes

Rostanga pulchra, an orange sponge-eating dorid nudibranch, was first described in 1905 by molluscan biologist Frank Mace MacFarland in the publication *Opistobranchiate Mollusca from Monterey Bay, California and Vicinity*. MacFarland's description documents several anatomical features examined in this thesis, including caryophyllidia, radular morphology, and dorsal pigmentation. These traits remain central to species descriptions and have proven relevant in other cryptic species complexes (Muniaín et al., 2000; Innabi et al., 2023; Matsuda et al., 2017; Lindsay et al., 2016).

Caryophyllidia—dorsal sensory tubercles composed of a ring of upright calcified rod-like spicules surrounding a fleshy papula with a raised central apical knob—are frequently documented in species descriptions but remain poorly understood. Present in many members of the superfamily Doridoidea, MacFarland (1905, p. 105) briefly described *R. pulchra*'s caryophyllidia as "hispid papillae," covering the dorsal surface. He reported them as small and closely set, approximately 0.42 mm in height and 0.08 mm in diameter but did not provide much more resolution to be examined (MacFarland, 1905, p. 105). This microanatomy—spicules, apical knob, and papula—forms an important component of the morphological variation examined in this study.

Anatomical features such as epithelial covering of spicule and ciliation (Gosliner, 1994), which require scanning electron microscopy for observation, were not reported here. Caryophyllidia are also muscular, allowing extension of the papula beyond the spicule ring

(Foale and Willan 1987). Caryophyllidia's exact function remains undescribed, although they are generally reported as having sensory capabilities (Foale and Willan 1987).

Caryophyllidia—their height, spicule arrangement, and apical knob shape—can be diagnostic and are frequently documented in species descriptions (Muniaín et al., 2000; Innabi et al., 2023). Delineation of cryptic species using caryophyllidium height has been demonstrated in *Jorunna tomentosa* (Neuhaus et al., 2020), though few other studies have attempted to resolve cryptic complexes using this structure. Gosliner (1994) described substantial variation in caryophyllidial structure within *Rostanga*, suggesting that this character may provide useful morphological resolution within cryptic species complexes.

The radula, a feeding organ with microscopic teeth used for rasping and grazing, was also described by McFarland (1905) in the description of *R. pulchra*. Radulae are highly organized, possessing multiple rows of teeth that vary in size and shape depending on their position within the row. He specifically identified the inner pleural tooth, describing it as stout and slightly curved, forming a loose hook. On the inner edge of the hook, 8–11 denticles (pointed extensions giving the pleural tooth a serrated appearance) were identified (MacFarland, 1905, p. 120). Denticles were among the characters examined in this study, alongside hook length and additional quantitative measurements. Other teeth described include the inner lateral teeth and the marginal teeth. MacFarland (1905, p. 120) noted the wing-like shape of the inner lateral teeth base and the varied number of points of the marginal teeth, both examined in this study.

Central to molluscan taxonomy, the radula is featured in many species descriptions (Muniaín et al., 2000; Innabi et al., 2023; Matsuda et al., 2017). Tooth number per row, denticle number, and tooth morphology are frequently used in species delineation (Korshunova, 2017). Despite successful documentation of cryptic species delineation by radulae (Innabi, 2023;

Korshunova et al., 2019), other studies found radulae to be unreliable (Jörger et al., 2013). Mixed results have also been reported in dorids, with radular characters being distinctive only when analyzed relative to body size (Stephen & Bloom, 1977). Notably, radular morphology can shift in response to diet and substrate (Jensen, 1993; Reid et al., 1999), introducing potential plasticity. Because prior studies indicated overlapping diets among OTUs (Fox, 2024), radular plasticity was not treated as a major confounding variable in this study.

Radular formulas, which describe the number and arrangement of teeth in a single transverse row, commonly facilitate interspecific comparisons; however, counts in *Rostanga* were often unreliable due to tightly packed marginal teeth and variable denticle numbers (Muniaín et al., 2000). Consequently, Muniaín et al. (2000) and others reported half-row counts excluding marginal teeth, a practice followed in this study.

Pigmentation patterns also contributed to species delineations. MacFarland (1905) documented much of the variation in dorsal mantle "minute spots" examined in this thesis. Minute spots were described as small brown or black spots located between caryophyllidia (MacFarland, 1905, p. 120). He also noted that minute spots could be aggregated into small patches or densely arranged (MacFarland, 1905, p. 120).

Spotting patterns have proven diagnostic in other cryptic complexes and species delineations; for example, molecular analyses resolving *Diaulula sandiegensis* into distinct species, revealed reliable differences in pigmented rings and spots (Lindsay et al., 2016). Prior work (Fox, 2024; Moreira-Andrade, 2024) indicated that OTU1 exhibited distinctive large black spots (actually round collections of minute spots), though increased sampling was recommended. Color variation, and potentially the noted spots in *R. pulchra,* reflects dietary pigment

sequestration, as carotenoids and related compounds have been shown to correspond with those of consumed sponges (Anderson, 1971).

Egg size, usually reported as diameter, is another trait frequently cited in species descriptions, with great variation, ranging from diameter of 90 to 380 μm within single nudibranch genera (Hadfield & Switzer-Dunlap, 1984). Although rarely used diagnostically due to sampling challenges, egg size provides information on maternal investment and larval development (Trickey et al., 2013; Marshall et al., 2012). MacFarland's original description did not mention eggs or egg masses; however, a previous study reported an egg diameter of 73 μm for *R. pulchra* (Anderson, 1971). Without OTU-level resolution, the applicability of this measurement is limited. Together, these traits represent the primary morphological characters historically used in species descriptions and delineations of *Rostanga* and related dorids.

Existing Literature on *Rostanga pulchra*

As this cryptic species complex has never been formally described, published species-level literature directly addressing this complex does not exist. However, Dr. Richard Emlet, at the Oregon Institute of Marine Biology, has facilitated several undergraduate studies investigating this system following his 2018 discovery of three genetically distinct species via molecular data.

One such study, *One Nudibranch One Sponge? Using Genetic Barcoding to Analyze the Rostanga pulchra Species Complex and Prey Differentiation* (Fox 2024), investigated dietary niches within the complex by identifying the orange sponge species on which *Rostanga pulchra* feeds. The data show overlapping levels of dietary selectivity among OTUs. In another study

facilitated by Emlet, Yvonne Moreira-Andrade collected additional dietary data demonstrating that all three OTUs feed on *C. pennata*.

Moreira-Andrade and Emlet also reported egg sizes among OTUs. Their findings suggested possible differences in egg diameter; however, sample sizes—particularly for OTUs 1 and 2—were limited. The present thesis expands this egg dataset to clarify whether egg size differs among OTUs.

Emlet also aided in preliminary data collected by Jackson Tisdale, using scanning electron microscopy (SEM) to document radular morphology. However, the sampling was incomplete and did not comprehensively represent all three OTUs. One radula prepared by Tisdale is incorporated into this thesis alongside newly prepared specimens.

Apart from the original description, Schrödl and Grau (2006) redescribed *R. pulchra* based on a single specimen from Ipún Island, Chile, and compared northern and southern hemisphere specimens using existing literature (MacFarland 1905; Marcus and Marcus 1969; Marcus 1969; Muniaín & Valdés 2000; Schrödl 2003). They examined coloration, rhinophoral lamellae, caryophyllidium morphology (including spicule number and apical knob shape), radula morphology, and reproductive anatomy. Despite this comprehensive approach, they reported no consistent morphological differences between hemispheres. Current molecular sequence data in BOLD (Barcode of Life Database), however, suggest that Chilean individuals represent a fourth OTU distinct from the three northeastern Pacific OTUs. Schrödl and Grau noted substantial variation in radular half-row counts, innermost lateral tooth serration, and marginal tooth structure. Their redescription supplemented the original description with SEM imagery but did not overturn earlier morphological conclusions from the original description. In the present study, comparisons with the Chilean OTU were not conducted due to a lack of living material.

Muniaín & Valdés (2000), cited by Schrödl and Grau (2006), compared *Rostanga byga* and *R. pulchra*, arguing that the two are readily distinguishable morphologically. Schrödl and Grau (2006), however, re-evaluated this claim and concluded that the most reliable differences were the presence of white dorsal dots, rhinophore lamellae counts, and subtle differences in reproductive anatomy. Although reproductive structures and rhinophoral lamellae were not examined here, several previously unexplored morphological traits were assessed. Regardless, Schrödl and Grau (2006) illustrate the taxonomic complexity within *Rostanga*, though their conclusions rely heavily on literature.

Garovoy et al. (2001) conducted a morphological analysis and identified sister clades consistent with geological isolation. *R. pulchra* was placed within a monophyletic clade alongside *R. byga* and *R. rubra*, species distributed in the Atlantic and eastern Pacific. Additional phylogenetic analyses have grouped *Rostanga* within a monophyletic assemblage of caryophyllidia-bearing dorids (Valdés and Gosliner 2001). While taxonomically informative, these broader phylogenetic findings are of limited direct utility for resolving the present cryptic complex.

More recently, Fernández-Vilert et al. (2025) expanded upon Garovoy et al. (2001) through extensive molecular analysis of Discodorididae, sequencing 142 taxa, including six *Rostanga* species. Their phylogeny, supported by bootstrap values >80 and posterior probabilities >0.8, suggests that *Rostanga* is likely polyphyletic. The study reorganized discodoridid relationships, reassigned select species (e.g., *Rostanga poddubetskaiae* transferred to *Doris*), and identified multiple cryptic species complexes. This broader phylogenetic instability further contextualizes the unresolved nature of the *R. pulchra* complex. Although a substantial body of literature exists on *Rostanga pulchra* and related taxa, comparatively little

work has examined variation at the OTU level, leaving the lineages within this cryptic complex poorly characterized.

Species Delineation Relevance

Accurate biodiversity estimation depends fundamentally on reliable species delineation. Without recognition of cryptic species complexes, biodiversity is systematically underestimated, obscuring true species richness and patterns of endemism. By documenting cryptic diversity, researchers not only increase recognized species counts directly, but also refine broader estimates of undiscovered diversity within a clade (Bickford et al., 2006). Furthermore, establishing morphological diagnosability within cryptic taxa—thereby rendering them pseudocryptic—creates a replicable framework for resolving additional complexes (Matsuda and Gosliner, 2017), compounding improvements in biodiversity again. This is particularly relevant in nudibranchs, where biodiversity is frequently underestimated; the suborder Doridina (inclusive of *Rostanga*) has been identified as one of the most taxonomically underestimated groups of sea slugs (Fernández-Vilert et al., 2025).

Conservation strategies rely upon accurate biodiversity and species knowledge. When cryptic diversity remains unrecognized, management plans risk overlooking distinct evolutionary lineages that may require independent protection. Bickford et al (2006) mentions numerous case studies where cryptic species complexes cause issues in conservation through the incorrect identification of a threatened species, the incorrect identification of a harmful species, the application of the wrong species as a biological control, or the reintroduction of the wrong species. Overall, a precise understanding of species boundaries therefore strengthens conservation planning by aligning management strategies with biological reality.

Refinements in biodiversity, as an indicator of environmental health, carry direct implications across a multitude of related fields. On their own, however, nudibranchs can serve as an indicator of environmental health, as many species, *R. pulchra* included, are stenophagous, or specialists eating few species, meaning that they may be used directly as a means to monitor health of specific populations (Todd 2001). Todd (2001) suggests that the abundance of nudibranchs and their dietary selectivity make them an underutilized indicator species.

Species delineation informs evolutionary interpretation. Robust phylogenetic resolution provides the foundation for understanding ecological specialization, niche partitioning, and lineage diversification. Integrating complete phylogenies with detailed morphological reassessment of cryptic complexes often reveals previously unrecognized mechanisms or adaptive pathways of speciation (Prieto-Baños 2025, Bickford et al., 2006). Importantly, recent work on dorid nudibranchs demonstrates that diversification patterns within clades are frequently associated with shifts in ecological and functional traits, including trophic specialization and secondary metabolite acquisition (Prieto-Baños 2025). Such findings underscore that resolving species boundaries is not merely taxonomic housekeeping, but foundational to interpreting trait evolution, lineage-specific ecological strategies, and macroevolutionary dynamics. By dissecting the morphological differences within the *Rostanga pulchra* cryptic species complex, this thesis contributes to a clearer evolutionary framework and establishes a foundation for future biological, ecological, and systematic research.

In marine systems, where biodiversity loss is accelerating, clarifying the true identity and distribution of prevalent organisms is increasingly urgent (Korshunova, 2017). Loss of valuable species-level knowledge through unrealized or fleeting diversity is a significant issue (Korshunova, 2017). Nudibranchs are of particular interest because of their often distinctive

chemical compounds, with biotechnology and pharmaceutical researchers exploring the unique array of bioactive metabolites synthesized by nudibranchs (Dean 2017). Doridoidea (inclusive of *R. pulchra*) is cited as the most chemically studied nudibranch superfamily (Dean 2017).

Accurate species delineation strengthens biodiversity estimates, refines conservation planning, holds unseen biochemical relevance, and clarifies evolutionary histories and trajectories. In the context of accelerating biodiversity loss, the value of accurately recognizing species diversity cannot be overstated. Moreover, with nudibranchs occupying distinctive highly specialized trophic links, their ecological importance can be directly assessed. Resolving cryptic diversity within groups such as the *Rostanga pulchra* complex, therefore, not only enhances systematic accuracy, but creates necessary building blocks for scientific advancement.

Methods

Specimen Collection

Rostanga pulchra were collected between 7/23/2025 and 11/24/2025 from multiple sites along Cape Arago (43.306221°N, -124.393452°W) near Coos Bay, Oregon. Collection occurred primarily at low tide, with additional samples obtained from floating docks in the Charleston (OR) Marina (43.3394318°N, -124.3239365°W). After initial surveys, rocks with overhangs were targeted because sponges were abundant in these high-flow, low-light environments. Red sponges (e.g., *Clathria pennata* and *Antho lithophoenix* sp.) were located on the undersides of these overhangs (Moreira-Andrade 2025), and careful examination of sponge surfaces revealed camouflaged nudibranchs. When specimens were located, the time and location of collection were recorded along with additional metadata when relevant. Specimens were placed in Eppendorf tubes half-filled with seawater and transported to the laboratory (Eppendorf, Hamburg, Germany). Because smaller nudibranchs rarely laid eggs in captivity, individuals smaller than 7 mm were excluded from later collections to improve sampling efficiency. In the laboratory, specimens were transferred to mesh baskets labeled with an assigned ID number and maintained in a shaded, flow-through tank. Specimens were monitored daily and provided fresh sponge as needed.

Morphological Surveys

Morphological observations were conducted under a dissecting microscope at a range of magnifications. Live specimens were placed in a small dish of water and illuminated laterally. The morphological survey followed the protocol outlined in Table 1. For variable traits, particularly those defining caryophyllidia, a fixed number of structures were examined (Table 1),

and the most common state was recorded. Measurements were assigned to bins based on ranges because exact measurements were not feasible for unanesthetized, highly motile organisms. Measurements were also defined relative to surrounding morphology, reflecting the comparative character descriptions commonly used in taxonomic keys. The same protocol was later applied to preserved specimens, which were observed in ethanol rather than water.

Q#	Question	Responses
	Caryophyllidia surveyed on the mid-dorsal region in front of the branchial plume (Fig 1.A.a). Observations were made on 10 caryophyllidia, and the most common response is used as the reported answer. Small underdeveloped caryophyllidia were excluded. Large caryophyllida directly boarding rhinophores and branchial plume were also excluded.	
1	Apical nub taller than surrounding papula?	1. Even in height with surrounding papula 2. height roughly half the width of surrounding papula 3. height greater than half the width of surrounding papula
2	Spicules taller than surrounding papula?	1. Below the surrounding papula 2. Even in height with surrounding papula 3. height roughly half the width of surrounding papula 4. height greater than half the width of surrounding papula
3	Spicules found embedded in between papula, or found more marginally?	1. Spicule circumference 0%-35% in contact with surrounding papula 2. Spicule circumference 35%-50% in contact with surrounding papula 3. Spicule circumference 50%-65% in contact with surrounding papula 4. Spicule circumference 65%-100% in contact with surrounding papula
	Minute spot aggregation and coloration surveyed on the entirety of the specimen's dorsal side (Fig 1.A.b). Aggregations are clusters of minutes spots.	

4	What is the variation in minute spots? Variation	1. no minute spots 2. 1-7 aggregation of minute spots 3. 7-20 aggregations of minute spots 4. 20 + aggregations of minute spots 5. heavy spotting with indistinguishable aggregations 6. heavily aggregated and dense minute spots that form distinct circular patches (refered to as large black spots)
	Branchial Plume (Fig 1.A.c)	
5	What is the branchial plume gill leave shape?	1. Straight 2. Minor waves 3. sharp kinks
6	What is the number of gill leaves in the branchial plume tree?	Numeric answer
	Marginal caryophyllidia to be surveyed from the marginal sections of the dorsal side of the dorid, in the central region of either flank (roughly in line with transverse plane) (Fig 1.A.d). The reported answer should be reflective of observations made on 10 caryophyllidia, where the most common response is used as the reported answer.	
7	Is the apical nub taller than surrounding papula?	1. Even in height with surrounding papula 2. height roughly half the width of surrounding papula 3. height greater than half the width of surrounding papula
8	Are the spicules taller than surrounding papula?	1. Even in height with surrounding papula 2. height roughly half the width of surrounding papula 3. height greater than half the width of surrounding papula
9	What is the relative height of caryophyllidia around rhinophores? To be sampled from caryophyllidia directly surrounding the rhinophores *(Fig 1.A.e)*.	1. Caryophyllidia equal in height to caryophyllidia not surrounding rhinophore 2. caryophyllidia roughly a paula width taller than caryophyllidia not surrounding rhinophore 3. caryophyllidia greater than a papula width taller than caryophyllidia not surrounding rhinophore

10	Relative height of caryophyllidia around the branchial plume? To be sampled from caryophyllidia directly surrounding the branchial plume *(Fig 1.A.f)*.	1. Caryophyllidia equal in height to caryophyllidia not surrounding branchial plume 2. caryophyllidia roughly a papula width taller than caryophyllidia not surrounding branchial plume 3. caryophyllidia greater than a papula width taller than caryophyllidia not surrounding branchial plume
11	Mantle rim organ developed or patchy? To be on the margin in the central region of either flank (roughly in line with the transverse plane) *(Fig 1.A.g)*.	1. Mantle rim organs are well developed even in size and spacing 2. Mantle rim organs appear patchy with uneven spacing and irregularity in size
12	Length of organism in mm	Numeric answer

Table 1: Morphological survey questions and responses

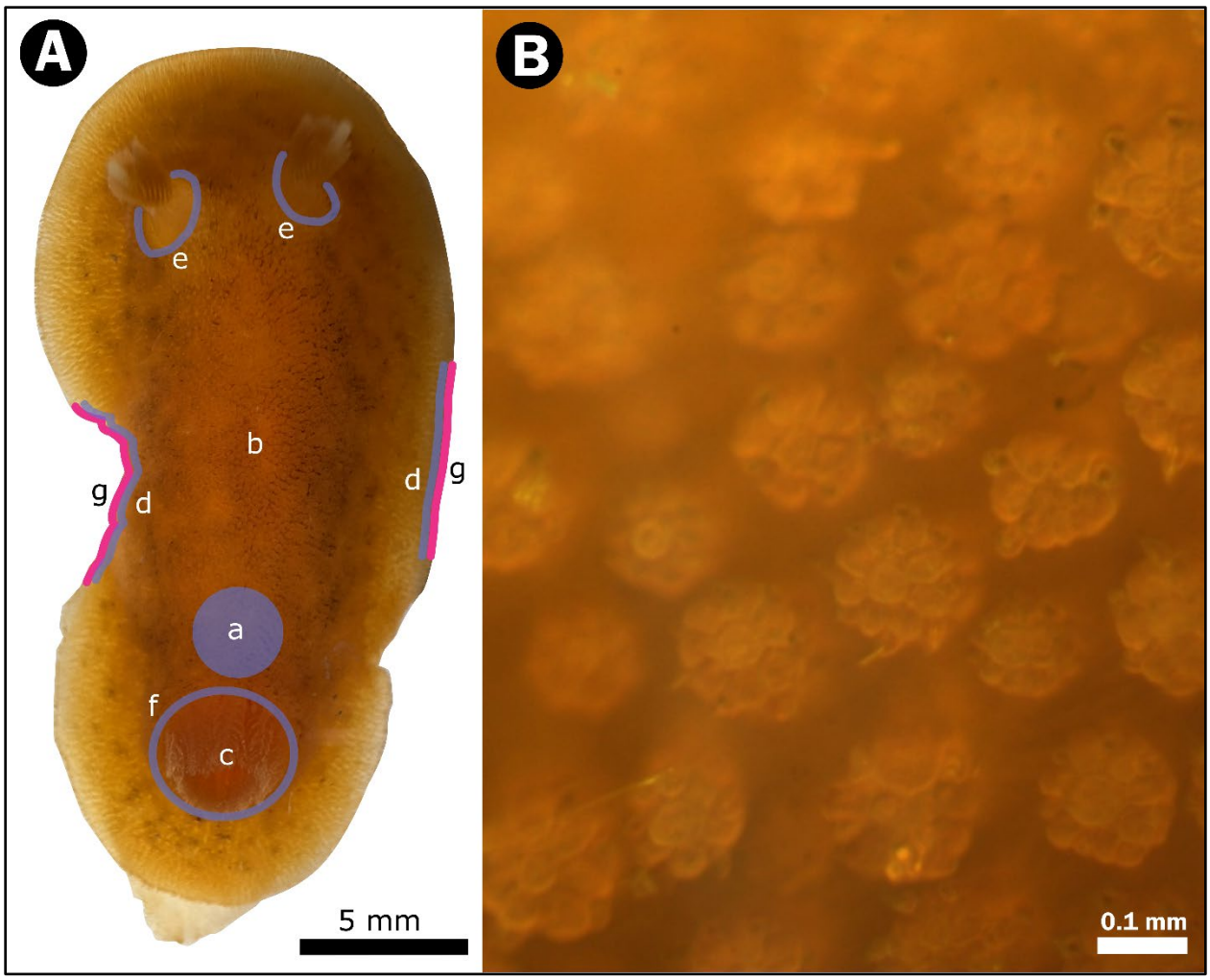

Figure 1: External morphological survey guide

A) Dorsal view of *Rostanga pulchra* with sample regions labeled. Photo of specimen W73, OTU2. a) The mid-dorsal region in front of the branchial plume, where caryophyllidia were surveyed in questions 1-3. b) Dorsum from which minute spots aggregation was surveyed in question 4. c) Branchial plume surveyed in questions 5 and 6. d) Marginal region from which caryophyllidia were surveyed in questions 7 and 8. e) The region surrounding the rhinophores where caryophyllida are surveyed in question 9. f) The region surrounding the branchial plume where caryophyllidia were surveyed in question 10. g) The marginal region where mantle rim organs were surveyed in question 1. 1.B) View of caryophyllida seen at 6.3x on specimen W37, OTU 3.

Radula Dissection:

Radula extraction followed the method of Gannon (2023). Specimens were anesthetized in 7.5% MgCl for 40–60 min until fully relaxed and immobile, then positioned ventral side up under a dissecting microscope. Radular inversion was performed using two blunt-ended or

rounded-tip tools. One tool was applied at the posterior of the foot to stabilize the specimen while firm, but gentle pressure was maintained, as damage to the foot or internal digestive tract during stabilization made extraction difficult. If reflexes were triggered during this step, such as the foot curling around the tool, the specimen was returned to anesthetic for an additional period.

With the slug firmly held in place, the second blunt-ended tool was positioned anterior to the first and moved up the length of the foot toward the head. This caused increased hydrostatic pressure in the intestines, along with increased physical pressure of the tool against the musculature. Increased pressure forced the radula to extend out of the mouth. When this stroking action was first performed along the length of the foot, the tool was not drawn all the way to the mouth of the organism, stopping 1–3 mm before to prevent internal damage to the radula. Care was also taken not to press too hard, which could damage internal organs or other features of the organism intended to remain visible for preservation.

After the first 10–15 strokes, the anterior portion of the foot appeared significantly inflated. This region of inflation was forced further toward the anterior end of the organism, such that the folds around the mouth began widening. Between approximately 15–30 strokes, with pressure focused more anteriorly, a muscular tube extended from the mouth of the slug. At this stage, steady pressure was maintained to keep the retractor muscles extended. Although the radula was likely contained within the now-visible buccal mass, it was too early to dissect. Continued stroking along the length of the foot was required, resetting the tool position after each stroke. Debris expelled during this process was removed with a pipette as necessary.

Between 30–45 strokes, the radula began to invert from within the buccal mass. Stroking continued until the radula was fully inverted. Once a deep medial groove surrounded by a region devoid of teeth was visible, dissection was possible. The buccal mass was grasped firmly just

below the radula with forceps, and a sharp blade was used to slice below the forceps, freeing the radula. Approximately 2 mm of buccal mass was left attached, and any excess tissue was trimmed. The radula was preserved in 70% ethanol and stored refrigerated following extraction.

Radula Scanning Electron Microscopy Preparation

The extracted radula was cleaned to remove organic material lodged between the teeth. Holding the buccal mass, the radula was immersed in 50% bleach for approximately 1 min, then removed and rinsed with deionized water from a squeeze bottle or gentle stream. The radula was oriented into the water stream to prevent partially dissolved buccal tissue from being deposited onto the teeth. The radula was transferred to a clean scintillation vial containing 10 mL of 10% buffered formalin and fixed for 1 h.

After fixation, the radula was removed with forceps or a wide-mouth pipette while minimizing excess fluid transfer. The fixed radula was placed in a clean beaker containing 15 mL of filtered seawater and left for 15 min. The rinse was repeated once with fresh filtered seawater.

The radula was transferred to a lidded bottle containing freshly prepared 2% OsO_4 in seawater. The sample was post-fixed for 1 h. The radula was removed and allowed to sit in reverse-osmosis (RO) water for 15 min, after which the sample was removed, moved to a clean bottle, and covered with 30% ethanol, starting the alcohol dehydration ladder. After 30 min, the sample was transferred sequentially to 50% ethanol for 30 min. The series continued with 70% ethanol for 30 min followed by 95% ethanol for 1 h then 100% ethanol for at least 1 h. Next, the radula was removed from the alcohol and put into a fresh bottle and covered with hexamethyldisilazane (HMDS). This bottle was left uncovered in the fume hood for 10 minutes.

The radula was then removed with a wide-mouth pipette, put into a shallow dish, and covered gently, allowing the remaining HMDS to evaporate. This took 10–20 minutes.

Dried radulae were highly susceptible to static and required extreme care when handling. Under the dissecting microscope, a carbon tape tab was applied to an SEM stub. The radula was carefully mounted on the stub using forceps and placed at a slight angle such that the medial groove and the SEM stub surface made a rough 30° angle. This orientation improved visualization of pleural tooth denticles. SEM stubs were sputter-coated with gold using a Cressington 108Auto sputter coater.

Scanning Electron Microscopy & Photography

SEM observation and photography were conducted using a Tescan VEGA II, following the manufacturer's operating manual. Micrographs were obtained at a range of magnifications appropriate to the structures examined. Low-magnification images documented overall radular structure, while higher-magnification images captured inner pleural teeth, associated denticles, and other tooth types including marginal and inner lateral teeth. Scale bars are provided for all micrographs.

Radular Measurements

Radular measurements were obtained from SEM photographs. Images were imported into ImageJ and calibrated using the scale bar printed on each SEM image. When available, five teeth were measured for each radular character. Inner pleural and inner lateral teeth were sampled as close to the central rows of the radula as possible (Fig. 2.A). Inner lateral teeth were sampled from the third position (second inner lateral tooth) of central rows, as the first inner lateral tooth

is often underdeveloped (Fig. 2.A). Marginal teeth were sampled from the anterior region of the radula, approximately two to three rows above the final row of inner lateral teeth (Fig. 2.A).

Half-row counts, defined as the number of teeth in a row from the inner pleural tooth to the final inner lateral tooth, were recorded following the method of Muniain et al. (2000). Measurements taken included the angle of the inner pleural tooth base, length of the inner pleural tooth back nub, length of the inner pleural tooth hook, ratio of inner lateral tooth point lengths, number of points on marginal teeth, and half-row count.

The inner pleural tooth base angle was defined as the angle between the marginally facing and medial-groove-facing basal extensions (Fig. 2.B.c). Inner pleural tooth back-nub length was the length of the marginally facing basal extension, measured from the tip to the nearest point where the hook meets the base (Fig. 2.B.d). Inner pleural tooth hook length was the length of the raised finger-like extension of the tooth, measured from the distal tip to its point of attachment to the base farthest from the distal tip (Fig. 2.B.a).

The ratio of inner lateral tooth point lengths was calculated as the length of the winged base (from point tip to the center of the angle where the hooked extension meets the base) divided by the length of the large hooked extension of the inner lateral tooth (from its distal tip to the center of the angle where the extension meets the base) (Fig. 2.A.e&f). Marginal tooth count was defined as the number of projections or denticles arising from a single marginal tooth (Fig. 2.C).

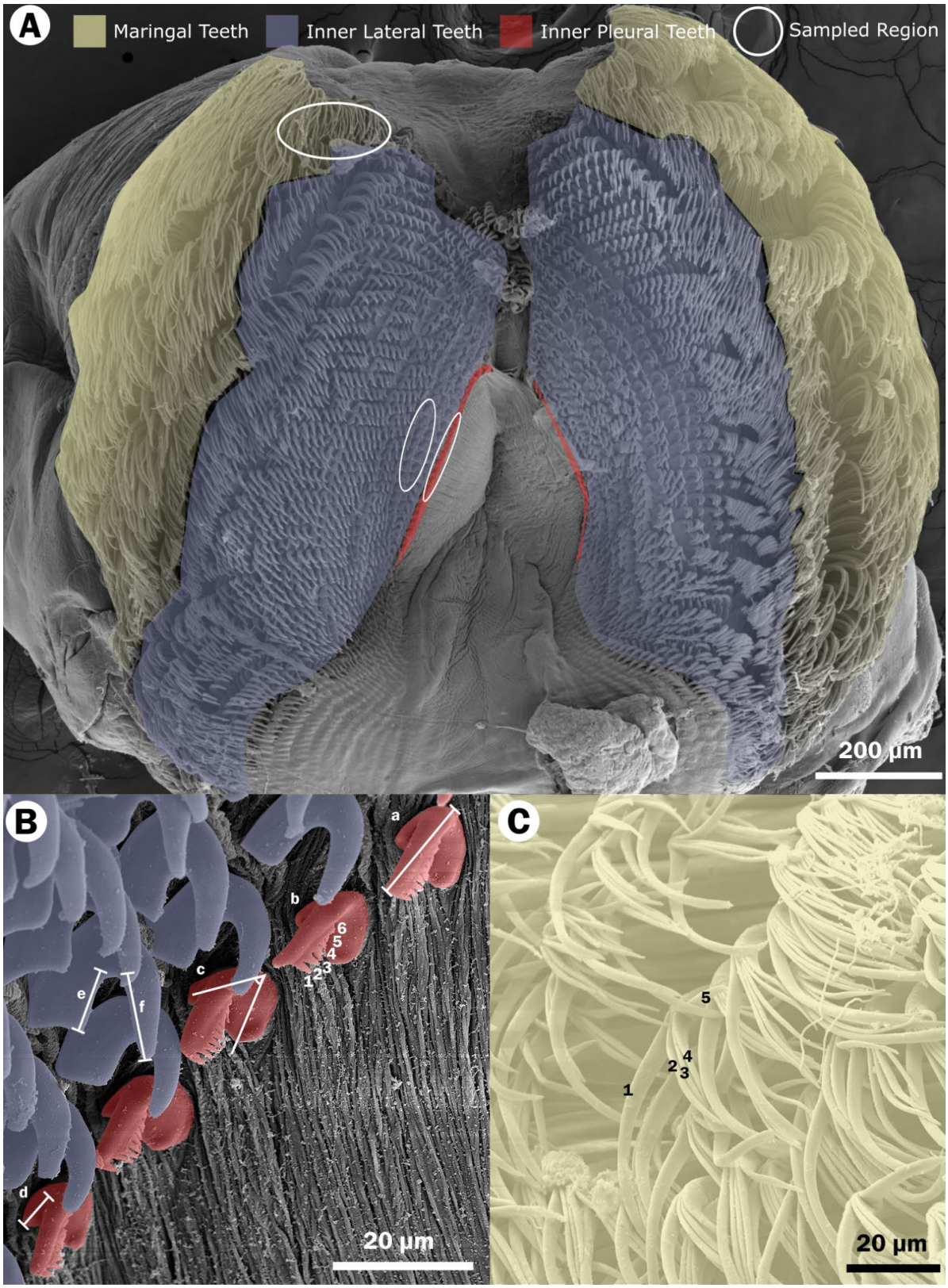

Figure 2: Radula characteristics guide

A) View of full radula. Different teeth are shapes with colors as follows. Marginal teeth, yellow; inner lateral teeth, blue; inner pleural teeth, located along red line. The ellipses show the sampled regions (Image of OTU1, W70). B) View of inner pleural teeth and inner lateral teeth with five characters shown: a) length of inner pleural tooth hook, b) count of inner pleural tooth denticles, c) angle of inner pleural tooth base, d) length of the inner pleural tooth back nub, e) length of the inner lateral tooth short point length, which when put in a ratio with f) length of the inner lateral tooth long point, gives a length ratio of inner lateral tooth point length (=e/f). (Image of OTU2, W72) C) View of marginal teeth from the anterior region of the radula. Numbers identify an example count of marginal teeth points (= splits) shown (Image of OTU3, W48).

Egg Diameter Measurements

Specimens housed in the flow-through tank were monitored daily. When egg masses were discovered, a 2–5 mm strand was removed from the mass using fine-tip forceps. The time of extraction and observations regarding the positions of both the egg mass and the nudibranch within the tank were recorded. Egg mass samples were placed on a glass slide in a drop of seawater and covered with a glass coverslip supported by clay feet to prevent compression of the eggs. Egg diameters were measured at 20× magnification on a compound microscope using an ocular micrometer (n = 25 eggs per sample). In some early samples, fewer eggs were measured. Only the egg cell was measured; the vitelline envelope and capsule were excluded. The ocular micrometer was not reoriented between measurements. If any eggs showed signs of cleavage, the entire egg mass was excluded from measurement. Ocular micrometer units were calibrated against a stage micrometer to the nearest micron.

DNA Extraction and Barcoding

A small section (~1 × 1 mm) from the posterior end of the foot was removed using sterilized fine-tip forceps and immediately preserved in 70% ethanol until DNA extraction. DNA extraction was performed using a Chelex-based method (InstaGene, BioRad) according to the manufacturer's protocol. PCR amplification was performed using the gastropod primers C_GasF1_t1 and C_GasR1_t1 (Steinke et al., 2016) and the universal COI primers LCO1490

and HCO2198 (Folmer et al., 1994). PCR amplification was performed using 4 µl of undiluted DNA in a Bio-Rad T100 Thermal Cycler (Bio-Rad Laboratories, Hercules, CA, USA) under the following conditions: 95°C for 2 min; 35 cycles of 95°C for 40 s, 45–52°C for 40 s, and 72°C for 1 min; and a 2 min final extension at 72°C. PCR products were purified using the Wizard SV Gel and PCR Clean-Up Kit (Promega, Madison, WI, USA). Purified PCR products were subsequently submitted to Eurofins Genomics LLC (Louisville, KY, USA) for bidirectional Sanger sequencing.

Phylogenetic Analysis

To assign specimens to molecular groups, COI sequences from the sampled individuals were analyzed together with a dataset of 68 previously barcoded specimens (Emlet, unpublished). A gene tree was constructed from the combined COI dataset (Fig. S1 in Supplemental Figures), and specimens were assigned to operational taxonomic units (OTU1–OTU3) based on their placement in the tree. Barcode Index Numbers (BINs) corresponding to each OTU were OTU1 = BOLD:ACB8198, OTU2 = BOLD:ACB7011, and OTU3 = BOLD:AAZ1998 (Emlet, unpublished).

Results

Phylogenetic Analysis

Genetic distances between groups (% nucleotide divergence across 650 bp of COI) were calculated as follows: OTU1–OTU2, 13%; OTU1–OTU3, 14%; and OTU2–OTU3, 11% (Emlet, unpublished). Of the 32 specimens included in the analysis, five belonged to OTU1, seven to OTU2, and 20 to OTU3 (Table 2). These counts represent the sample sizes used in the survey of external morphology. Radular characteristics and egg diameter measurements were obtained from smaller subsets of these individuals.

OTU Designation	Sample ID
1	W46
1	W47
1	W54
1	W52-2
1	W70
2	W49
2	W53
2	W51B-2
2	W73
2	W72
2	W75
2	W74
3	W30
3	W31
3	W34
3	W35
3	W36A
3	W36B
3	W37
3	W38
3	W44
3	W48
3	W52
3	W51
3	W50
3	W54b-2
3	W60
3	W61
3	W64
3	W63
3	W62
3	W71

Table 2: Phylogenetic designations

Molecular groupings of *Rostanga pulchra* based on partial sequences of mitochondrial COI gene. See full phylogenetic tree in Supplemental Figures, Fig. S1.

External Morphological Survey Overview

The external morphological survey examined a range of characters commonly used in species descriptions, as well as several less frequently used traits. Table 3 summarizes the surveyed characters and identifies those that differed significantly among OTUs based on a Kruskal–Wallis test followed by Dunn's post hoc test. Characters that did not exhibit statistically significant differences between OTUs based on a Dunn post hoc test are not discussed further in Results. An exception was made for apical knob height, which did not differ significantly but is included to provide a complete characterization of caryophyllidia.

Morphological Trait	**Kruskal-Wallis p-Value**	**Dunn p-values**		
		OTU1 - OTU2	**OTU1 - OTU3**	**OTU2 - OTU3**
Caryophyllidia spicule height on dorsum	*P*<.001	*P*<.001	.05	.04
Caryophyllidia spicule position on dorsum	*P*<.001	*P*<.001	.02	.001
Caryophyllidia apical knob height on dorsum	.08	—	—	—
Caryophyllidia spicule height on margin	.17	—	—	—
Caryophyllidia apical knob height on margin	.51	—	—	—
Minute spot aggregation	*P*<.001	*P*<.001	0.002	0.75
Branchial plume gill leaves count	.33	—	—	—
Branchial plume gill leaves shape	.74	—	—	—
Height of caryophyllidia	.90	—	—	—

around rhinophores				
Height of caryophyllidia around branchial plume	.25	—	—	—
Mantle rim organ highly developed or patchy	.16	—	—	—
Preserved caryophyllidia spicule height on dorsum	*P*<.001	*P*<.001	0.06	0.03
Preserved caryophyllidia spicule position on dorsum	*P*<.001	*P*<.001	0.09	0.01
Preserved caryophyllidia apical knob height on dorsum	.34	—	—	—

Table 3: Summary of morphological traits analyzed and their statistical significance

Identifies which traits from the survey of external morphology are statistically different at a significance level of $p \leq 0.05$ based on an initial Kruskal Wallis test and Dunn post hoc. Number of individuals surveyed was five OTU1, seven OTU2, and 20 OTU3.

Caryophyllidium Structure

Caryophyllidium structure, characterized by spicule height, spicule position, and apical knob height, was morphologically divergent between OTUs. Relative spicule height and spicule position differed significantly (Table 3). In contrast, relative apical knob height showed no statistically significant differences among OTUs (Table 3).

Relative spicule height differed most strongly between OTU1 and OTU2 (Fig. 3). OTU1 exhibited unique variation in spicule height, with three individuals possessing spicules shorter than the surrounding papula, a variant not expressed by any other OTU. The remaining two OTU1 specimens had spicules even with the surrounding papula (Fig. 3).

The majority of OTU3 individuals had spicules even with the papula (n = 14), whereas others had spicules extending half (n = 5) or more than half a papula width in height beyond the caryophyllidium surface (n = 1) (Fig. 3). Spicule heights in OTU2 overlapped with those of OTU3 but occurred at inverted frequencies, with spicules commonly extending more than half (n = 3) or half (n = 3) a papula width above the caryophyllidium surface (Fig. 3). One OTU1 individual also exhibited spicules even with the surrounding papula. These distributions differed significantly between OTUs (Table 3).

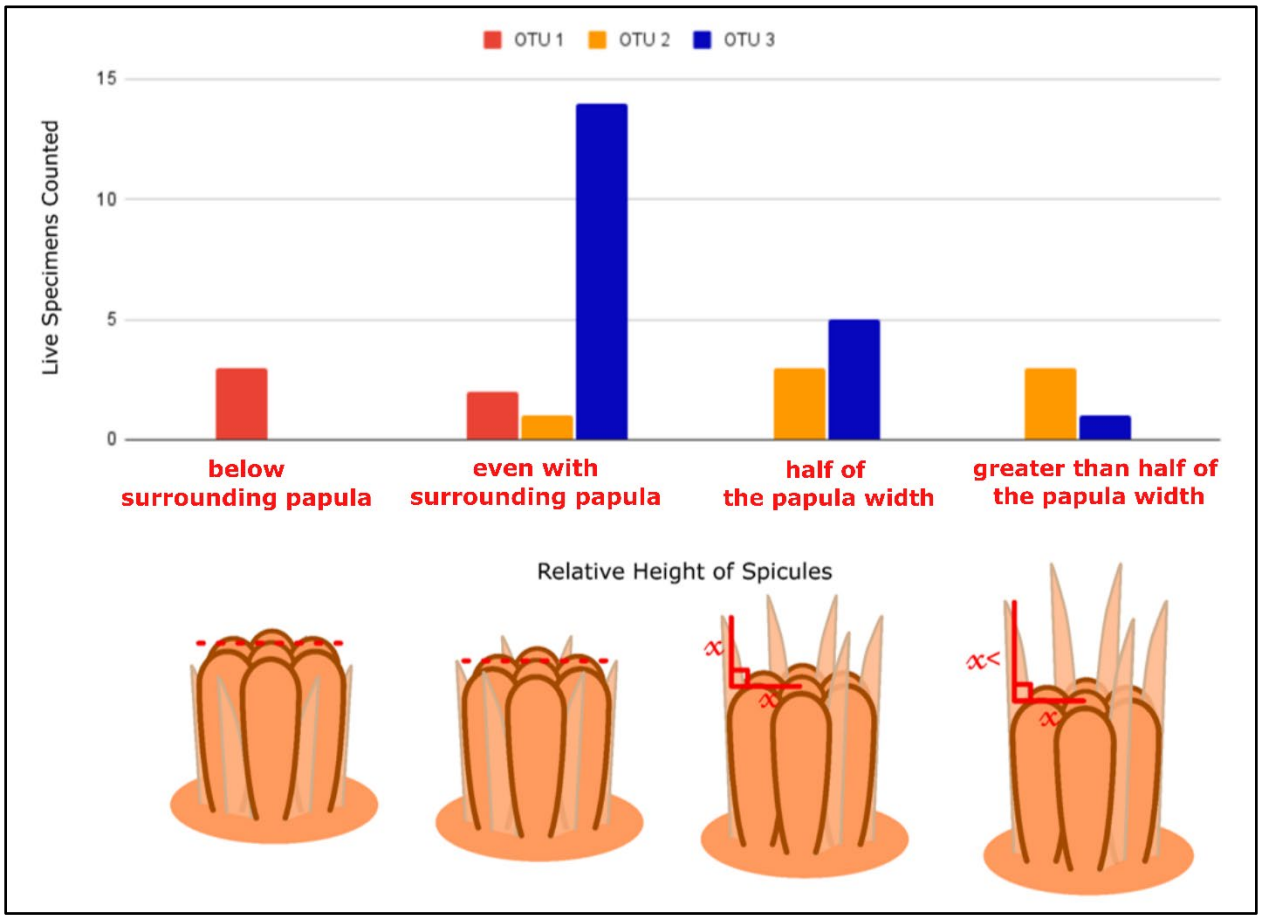

Figure 3: Relative spicule height of OTU1, OTU2, and OTU3

Bar graph showing the height of spicules relative to the width of the papula of the caryophyllidia (five OTU1, seven OTU2, and 20 OTU3 specimens), specimen designation based on the most common answer from 10 randomly selected caryophyllidia. Variance was recorded as spicules lying below the surrounding papula, being even with the surrounding papula, being half the caryophyllidium's papula width, or being greater than half the caryophyllidium's papula width.

Spicule position between the papula also differed significantly between OTUs with less overlap (Fig. 4). OTU2 was the most distinctive variant with a distal spicule position; all seven specimens had spicules positions with 35% or less of the spicule circumference contacting the papula (Fig. 4). OTU3 had the greatest range across categories of spicule position, but the majority (16 of 20) of individuals had spicules with 35%-50% of the circumference contacting surrounding papula (Fig. 4). Individuals in OTU1 had spicules deeply inset, with three of five having 65%-100% of their circumference in contact with the papula, and the other two individuals having 50%-65% in contact with papula (Fig. 4). These distributions differed statistically between OTUs (Table 3).

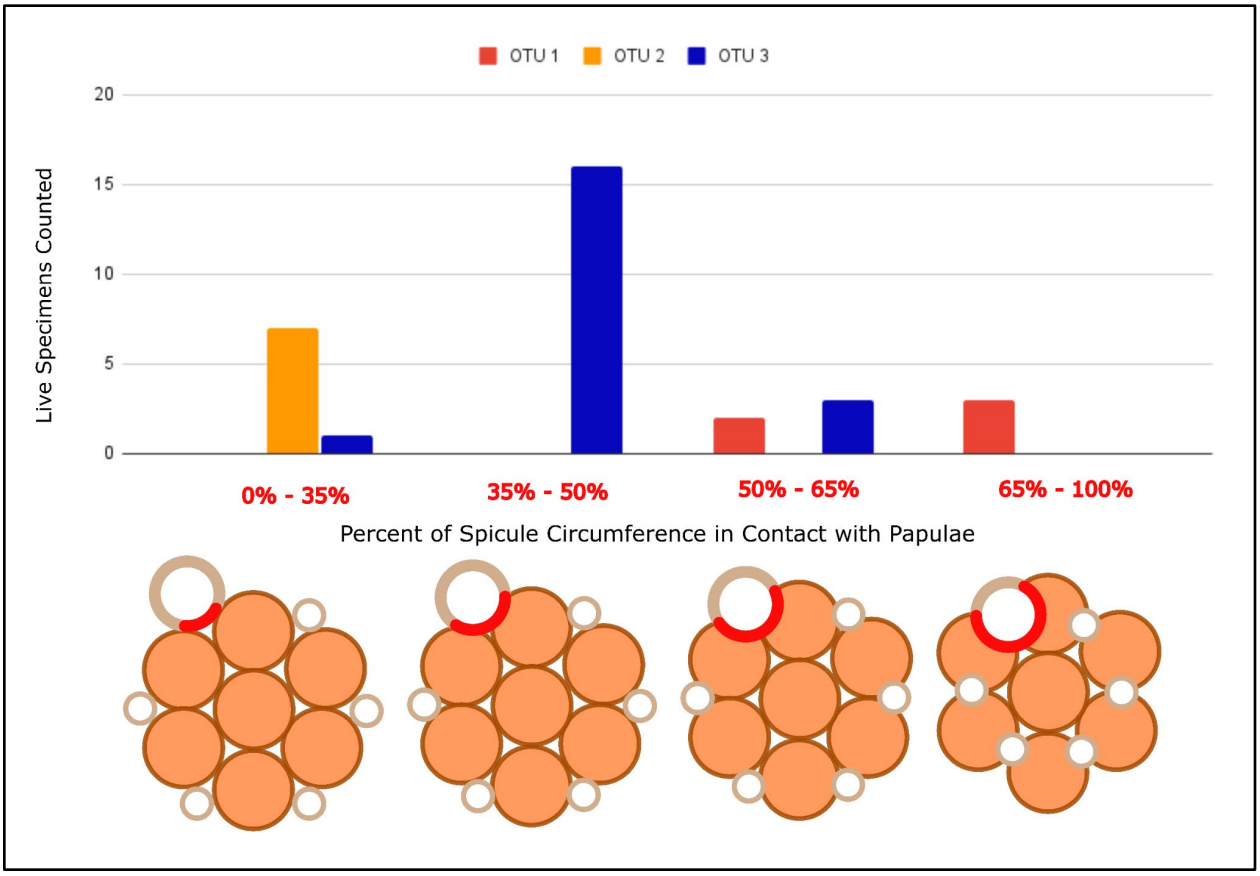

Figure 4: Spicule position of OTU1, OTU2, and OTU3

Bar graph showing the distribution of spicule positions for the three OTUs (five OTU1, seven OTU2, and 20 OTU3). Specimen designation based on the most common answer from 10 randomly selected caryophyllidia.

Variance was recorded as spicule circumference in contact with surrounding papula, with categories of 0%-35%, 35%-50%, 50%-65%, and 65%-100%.

Relative height of the apical knob varied among OTUs but did not appear to provide a statistically relevant character (Fig. 5). OTU1 exhibited the narrowest variance, with all observed specimens having an apical knob even with the surrounding papula (n = 5). OTU2 displayed a majority of specimens with the apical knob even with the surrounding papula (n = 4), although some individuals possessed apical knobs approximately half the papula width in height above the caryophyllidium surface (n = 3). OTU3 specimens exhibited the greatest variance in apical knob height. However, most specimens, similar to OTU1 and OTU2, had apical knobs even with the surrounding papula (n = 9), although some posed apical knobs extending half (n = 6), or greater than half a papula width (n = 5) above the caryophyllidium surface. No significance was seen in these distributions despite differing ranges.

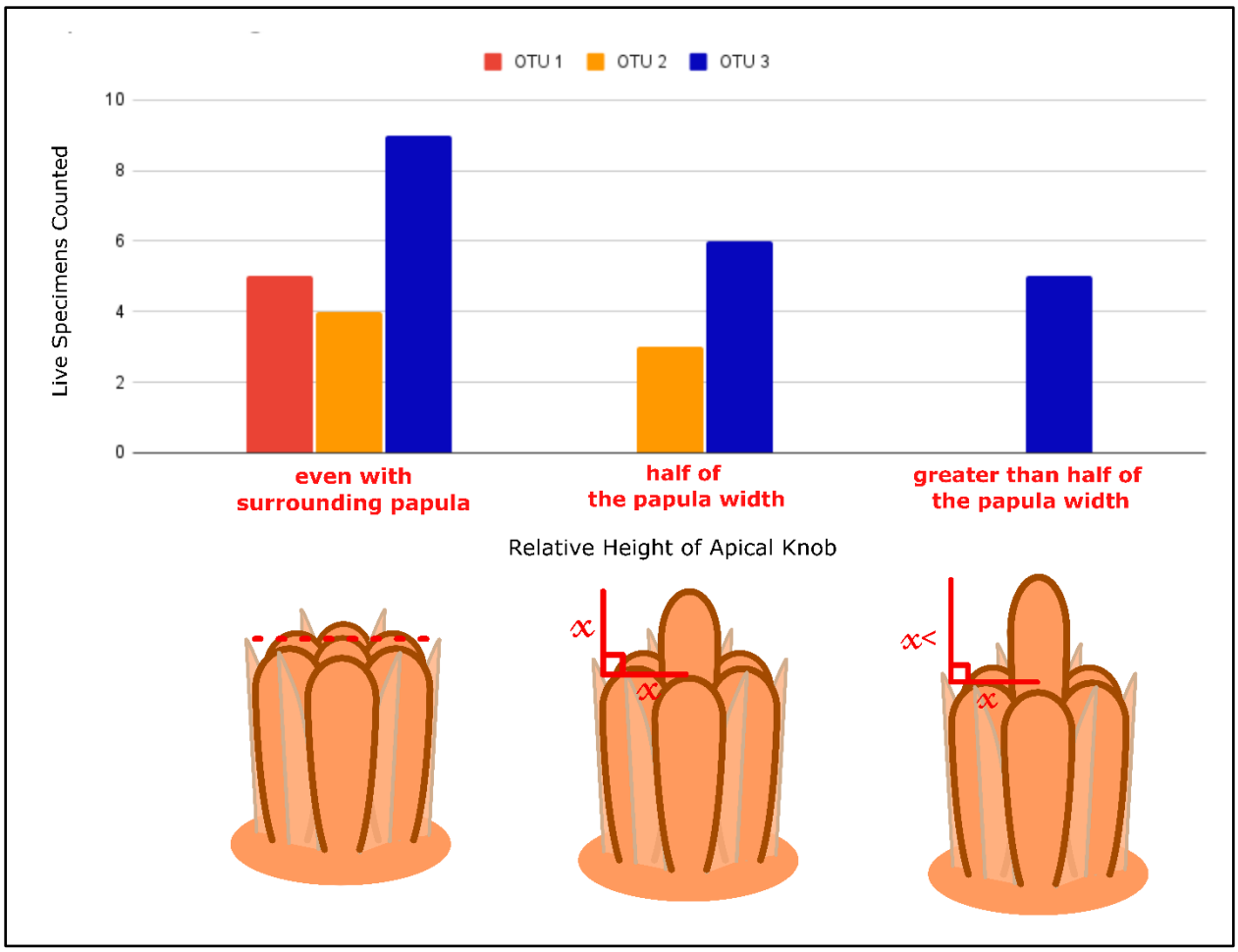

Figure 5: Relative apical knob height of OTU1, OTU2, and OTU3

Bar graph of height of the apical knobs relative to the width of the papula of the caryophyllidium (five OTU1, seven OTU2, and 20 OTU3 specimens). Specimen designation based on the most common answer 10 randomly selected caryophyllidia. Variance was recorded as being even with the surrounding papula, being half the caryophyllidium's papula width, or being greater than half the caryophyllidium's papula width.

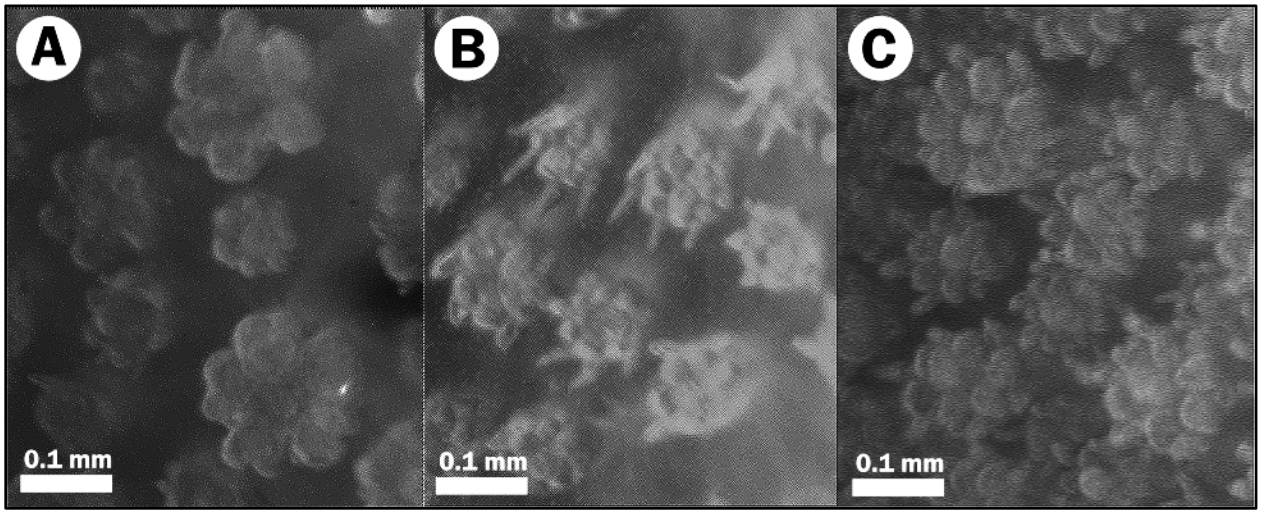

Figure 6: Light microscope photos of the caryophyllidia of OTU1 (A), OTU2 (B), and OTU3 (C).

A) Caryophyllidia of W70, OTU1. B) Caryophyllidia of W63, OTU2. C) Caryophyllidia of W63, OTU3.

Light microscopy photos highlighting the mentioned variation in caryophyllidium structure among OTUs are shown in Fig. 5. When all three measured caryophyllidial characters were examined together, OTU3 exhibited the greatest overall range of morphospace and shared the greatest overlap with OTU1 (Fig. 7). OTU2 occupied a comparatively narrow and distinct region of morphospace, with limited overlap with OTU3, and no overlap with OTU 1 (Fig. 7). OTU1 displayed the narrowest range of characters, with all individuals falling into two distinct morphologies represented by two clusters on the plot (Fig. 7).

To further evaluate these patterns, preserved specimens were surveyed using the same methodology. Spicule height, spicule position, and apical knob height varied in a similar way to those observed in live specimens but exhibited substantially greater overlap among OTUs (Fig. S2, S3, S4 In Supplemental Figures). Fig. 8, analogous to Fig. 7, displays all three measured caryophyllidial characters in combination for preserved specimens and illustrates the reduced variation among OTUs, as indicated by greater overlap of confidence ellipses. Statistical significance among OTUs decreased for all measured caryophyllidial characters except spicule height between OTU2 and OTU3, which retained a slightly lower p-value (Table 3). Differences in caryophyllidial characters between OTU1 and OTU3 were not statistically significant in preserved specimens (Table 3).

Figure 7: NMDS ordination of caryophyllidial characters for live OTU1, OTU2, and OTU3 specimens

Characters include spicule height, apical knob height, and spicule position (n = 5 OTU1, 7 OTU2, 20 OTU3). Each point represents a live specimen. Ellipses indicate 95% confidence intervals for each OTU. NMDS stress = 0.052.

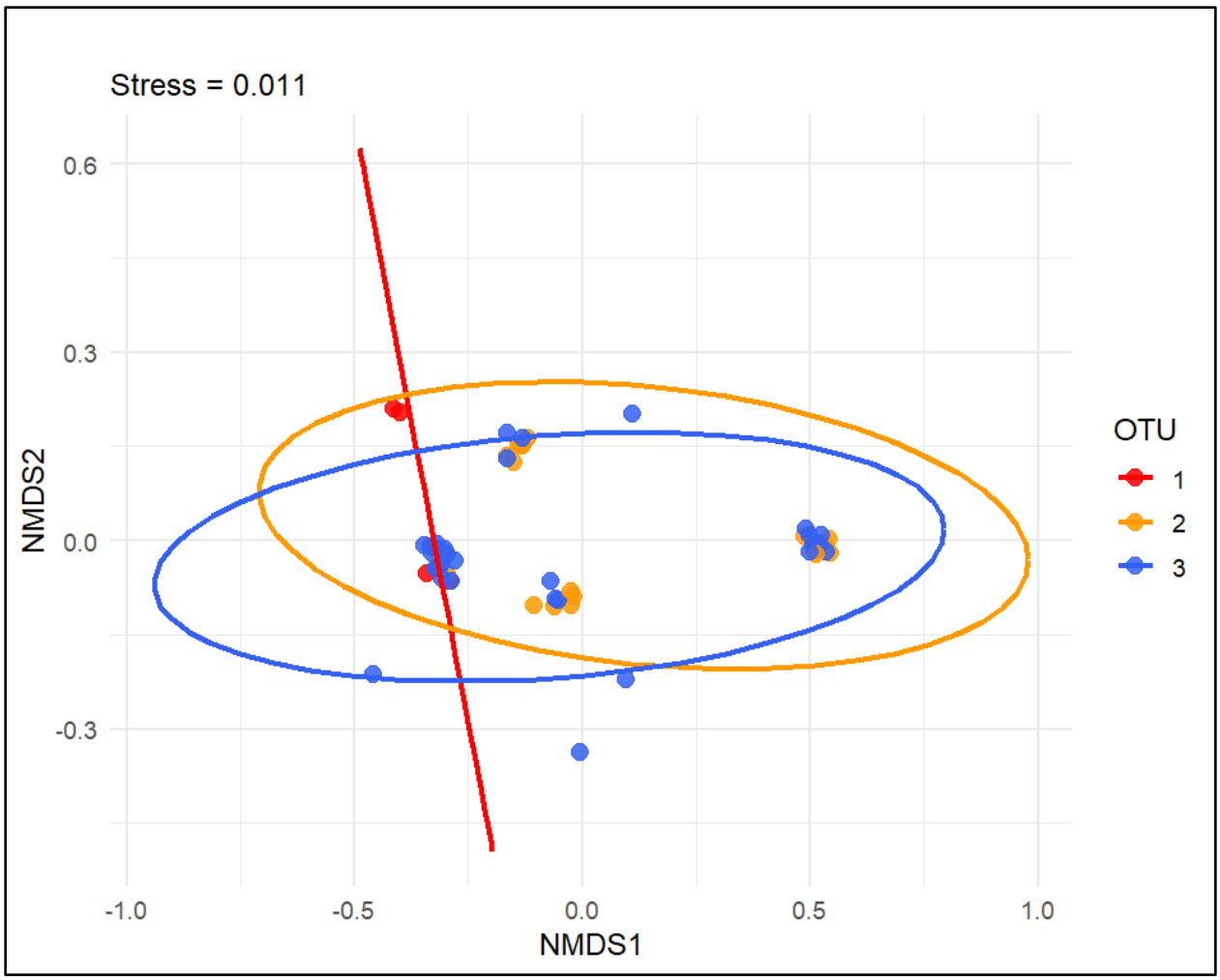

Figure 8: NMDS ordination of caryophyllidial characters for preserved OTU1, OTU2, and OTU3 specimens

Characters include spicule height, apical knob height, and spicule position (n = 4 OTU1, 19 OTU2, 31 OTU3). Each point represents a preserved specimen. Ellipses indicate 95% confidence intervals for each OTU. NMDS stress = 0.011.

Minute Spot Aggregation

Minute spots, were evaluated in the external morphological survey based on number of aggregations, defined as clusters of minute spots, and aggregation style. Within this framework, minute spots showed statistical divergence in OTU1 (Fig. 9, Table 3). Although OTU2 and OTU3 occupied different ranges of variation, the difference was not statistically significant (Fig. 9, Table 3).

OTU1 exhibited the most distinctive pattern of minute spots. All surveyed specimens (n = 5) display tightly aggregated minute spots forming distinct circular patches (referred to as large black spots) (Fig. 9). This trait was absent in other OTUs, providing a statistically significant diagnostic character (Table 3).

All but one OTU2 specimen (n = 6) lacked minute spots entirely. A single OTU2 specimen exhibited heavy spotting with indistinct aggregations, a variant not held by any other OTU (Fig. 9). OTU3 exhibits broad variation compared to the other OTUs, ranging from no minute spots (n = 8) to more than 20 aggregations (n = 2), with the frequency of specimens declines with increasing aggregation number (Fig. 9). Despite these differences between OTU2 and OTU3, statistical significance was not detected with current sampling (Table 3).

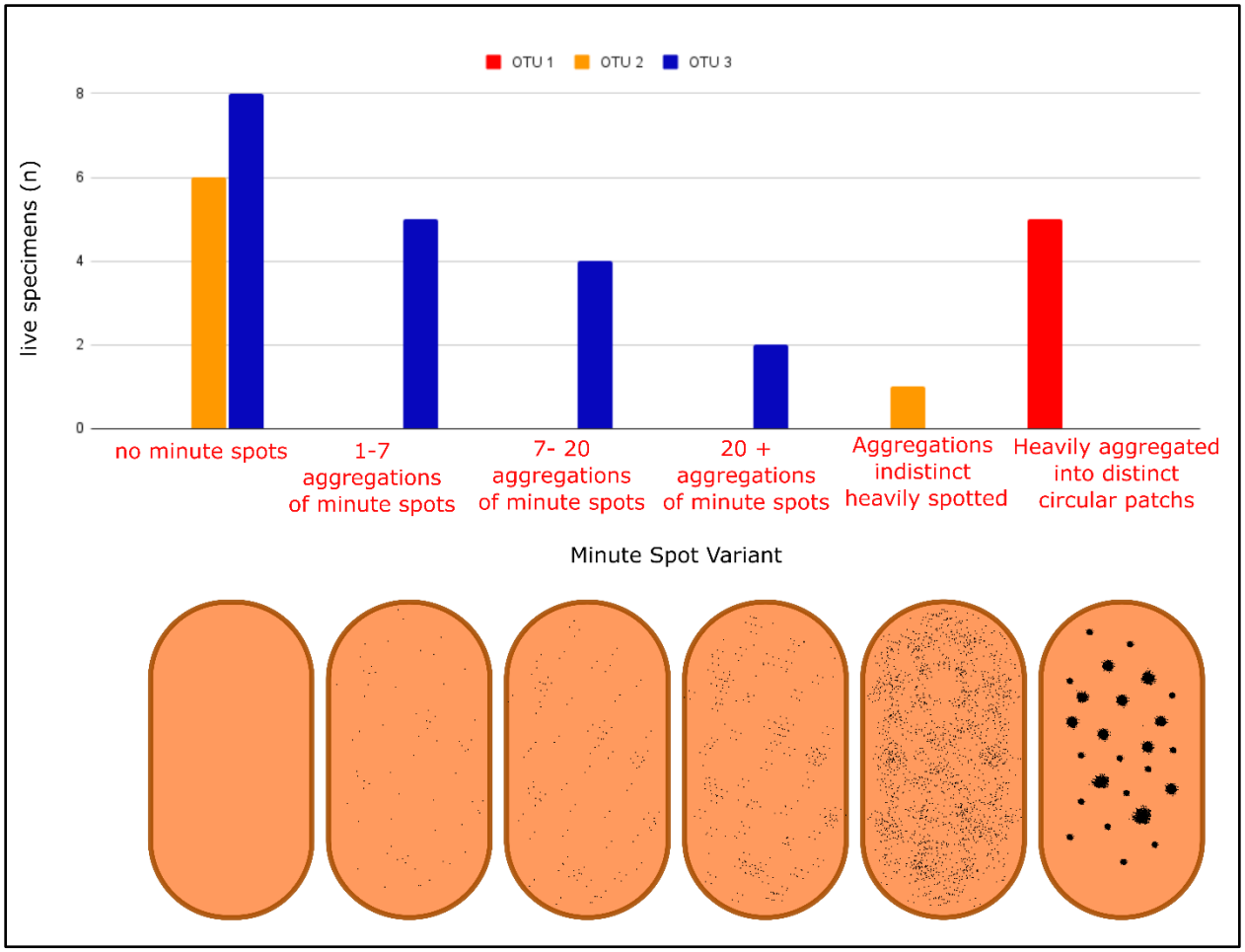

Figure 9: Minute spot density and aggregation of OTU1, OTU2, and OTU3

Bar graph showing the distribution of different categories of minute black spots on the dorsal surface of the nudibranchs five OTU1, seven OTU2, and 20 OTU3 specimens). Designations were based on full examination of dorsum at magnifications up to 10x. Variance was recorded as no minute spots, aggregations of 2-6 minute spots, aggregations of 7-20 minute spots, aggregation of 20 + minute spots, heavy spotting, aggregations indistinct heavily spotted, and tightly aggregated minute spots that form distinct circular patches (large black spot).

Overview of Radular Characteristics

Scanning electron microscopy (SEM) examination of radulae revealed a range of morphological characters, including both commonly used and less frequently reported traits in species descriptions and delineations. The statistical significance and diagnostic potential of these characters are summarized in Table 4. Characters that did not show statistical significance are not discussed further.

Radular Characteristic	**Kruskal-Wallis p-Value**	**Dunn p-values**		
		OTU1 - OTU2	**OTU1 - OTU3**	**OTU2 - OTU3**
Inner pleural teeth hook length	.44	—	—	—
Inner pleural teeth denticle count	.31	—	—	—
Inner pleural teeth base angle	.02	.02	.09	1
Inner pleural teeth back nub length	.02	.04	1	.047
Marginal teeth point count	.05	.047	.83	.43
Inner lateral teeth point length ratio	.02	.04	.05	1
,Half row count	.96	—	—	—

Table 4: Summary of radular traits analyzed and their statistical significance

Identifies which radular traits from scanning electron microscopy are statistically different at a significance level of $p \leq 0.05$ based on an initial Kruskal Wallis test and Dunn post hoc. Significant differences may be useful as a diagnostic trait. Number of individuals surveyed was four OTU1, five OTU2, and five OTU3

Inner Pleural Teeth

Four characteristics of the inner pleural teeth were measured, but only base angle and back nub length differed significantly between OTUs. Representative SEM photos of each OTU are shown in Fig. 10. Base angle (Fig. 2B.c) showed high divergence in OTU1, as it was consistently obtuse (mean = 151°), whereas the corresponding angle in other OTUs were more acute. OTU2 and OTU3 had mean base angles of 38° and 56°, respectively, and did not differ significantly (Fig. 11, Table 4). The distribution of base angles in OTU1 differed significantly from that of OTU2 but not from OTU3; however, the ranges of OTU1 and OTU3 did not overlap among examined specimens (Fig. 11, Table 4).

Back nub length of the inner pleural tooth—a measurement of the marginally facing basal extension (Fig. 2B.d; Fig. 12)—also differed significantly among OTUs (Table 4) with strong morphological divergence seen in OTU2. OTU2 exhibited a uniquely long back nub, with a mean length of 8 μm (Fig. 12). This value is approximately twice that observed in OTU1 and OTU3, which both had mean lengths of 4 μm (Fig. 12) and did not differ significantly from each other (Table 4). Differences in back nub length are also visible in Fig. 10.

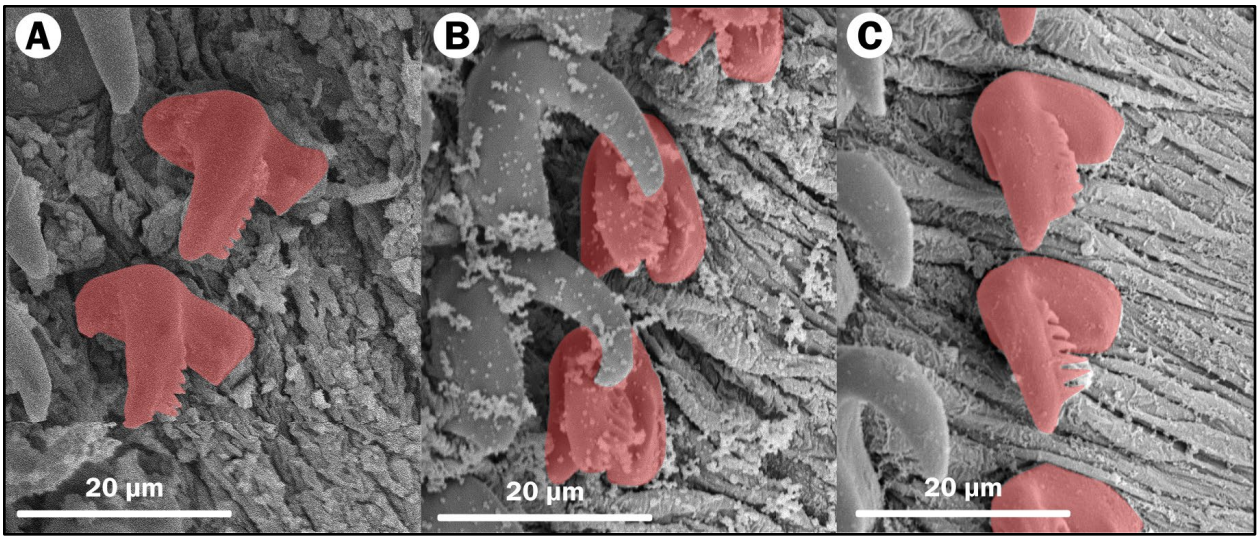

Figure 10: SEM photos of the inner pleural teeth of OTU1 (A), OTU2 (B), and OTU3 (C).

A) Inner pleural teeth of W47. B) Inner pleural teeth of J2. C) Inner pleural teeth of W60. J2 was collected and prepared by Tisdale (2024).

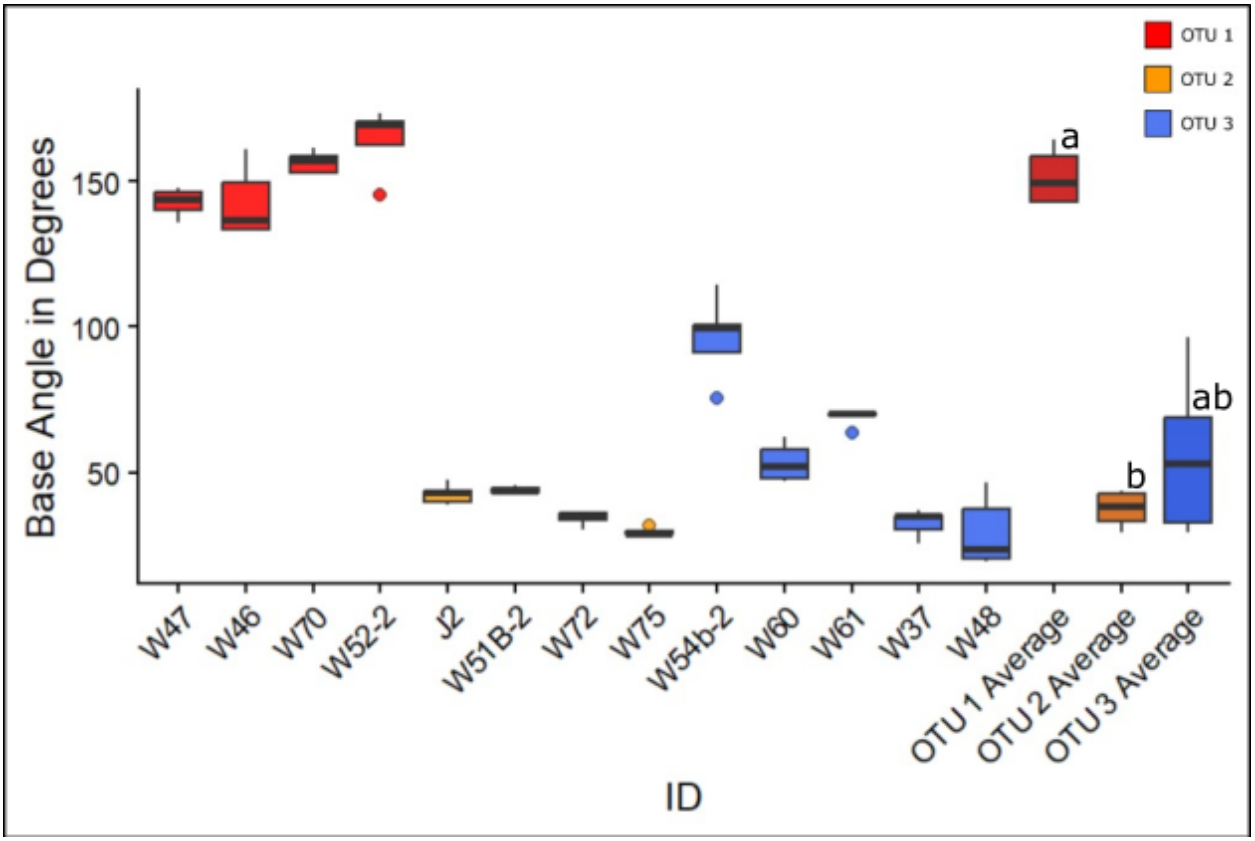

Figure 11: Box plots of inner pleural teeth base angle for OTU1, OTU2, and OTU3

Base angles (°) of five inner pleural teeth per specimen, found in central rows of the radula. Individuals with W prefix collected and barcoded for this investigation, J2 was barcoded previously and the radula prepared by Tisdale (2024). OTU # Averages (right side) are plots of all specimen's average base angle grouped by OTU.
Lower and upper box boundaries 25th and 75th percentile, respectively, line inside box median, lower and upper error lines furthest non-outlier point, colored dots outliers. Different letters above boxes indicate statistically significant differences among groups (Dunn's post hoc test following Kruskal–Wallis; $p < 0.05$). Groups sharing a letter are not significantly different. Inter-OTU Dunn test post hoc p-values are as follows: OTU1–OTU2: $P = .02$, OTU1-OTU3: $P = .09$, OTU2-OTU3: $P = 1$.

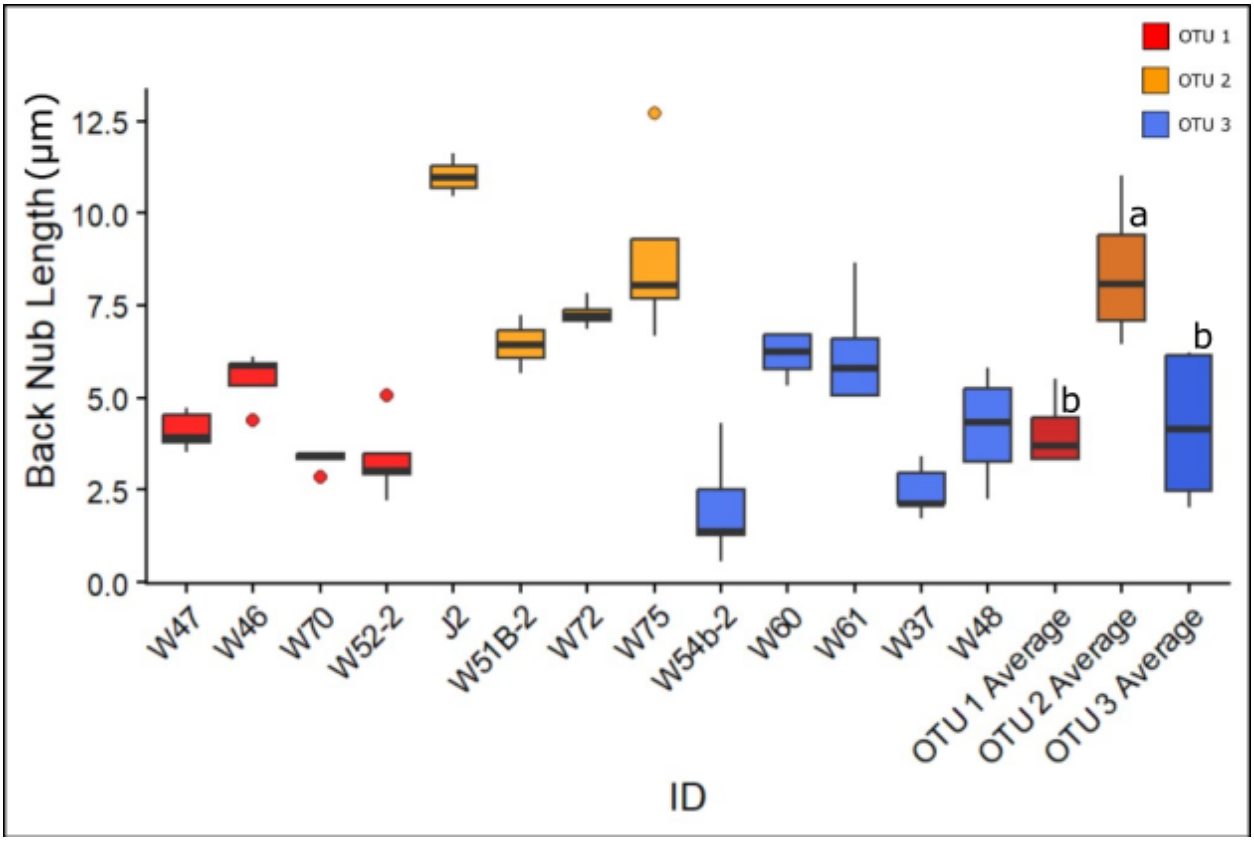

Figure 12: Box plots of inner pleural teeth back nub length (µm) for OTU1, OTU2, and OTU3

Back nub length (µm) of five inner pleural teeth, per specimen. Individuals with W prefix collected and barcoded for this investigation, J2 was barcoded previously and the radula was prepared by Tisdale (2024). OTU # Averages (right side of graph) are plots of all specimen's average back nub length grouped by OTU. Lower and upper box boundaries 25th and 75th percentile, respectively, line inside box median, lower and upper error lines furthest non-outlier point, colored dots outliers. Different letters above boxes indicate statistically significant differences among groups (Dunn's post hoc test following Kruskal–Wallis; $p < 0.05$). Groups sharing a letter are not significantly different. Inter-OTU Dunn test post hoc p-values are as follows: OTU1–OTU2: $P = .04$, OTU1-OTU3: $P = 1$, OTU2-OTU3: $P = .047$.

Inner Lateral Teeth

The ratio of inner lateral point lengths (Fig. 2.Be&f) differed significantly among OTUs and showed strong morphological divergence in OTU1. OTU1 exhibited the lowest ratio, with a

mean of 0.5 (Fig. 13). OTU2 and OTU3 had similar ratios, both averaged 0.8 (Fig. 13). Only the ratio observed in OTU1 differed significantly from those of the other OTUs (Table 4).

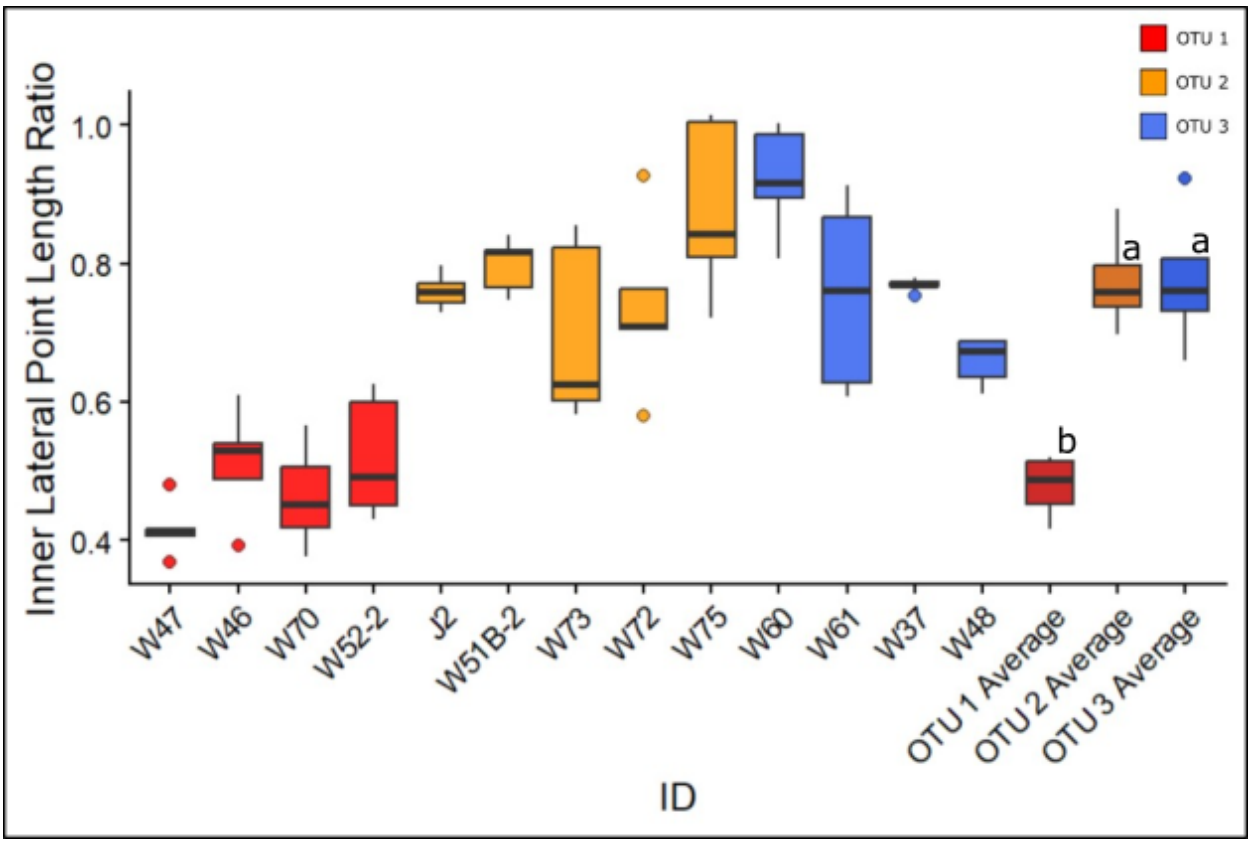

Figure 13: Box plots of inner lateral teeth point length ratio for OTU1, OTU2, and OTU3

Length ratio of the Point of five second inner lateral teeth, per specimen. Individuals with W prefix were collected and barcoded for this investigation, J2 was barcoded previously and prepared for SEM by Tisdale (2024). OTU # Averages (right side) are plots of all specimen's average length ratio of inner lateral points grouped by OTU. Lower and upper box boundaries 25th and 75th percentile, respectively, line inside box median, lower and upper error lines furthest non-outlier point, colored dots outliers. Different letters above boxes indicate statistically significant differences among groups (Dunn's post hoc test following Kruskal–Wallis; $p < 0.05$). Groups sharing a letter are not significantly different. Inter-OTU Dunn test post hoc p-values are as follows: OTU1–OTU2: $P = .04$, OTU1-OTU3: $P = .05$, OTU2-OTU3: $P = 1$.

Marginal Teeth

Marginal tooth point counts (Fig. 2C) differed significantly only between OTU1 and OTU2, showing limited morphological divergence. No significant differences were detected between OTU2 and OTU3 or between OTU1 and OTU3 (Table 4). Mean point counts for OTU1,

OTU2, and OTU3 were 2.8, 5.1, and 3.9, respectively (Fig. 14).

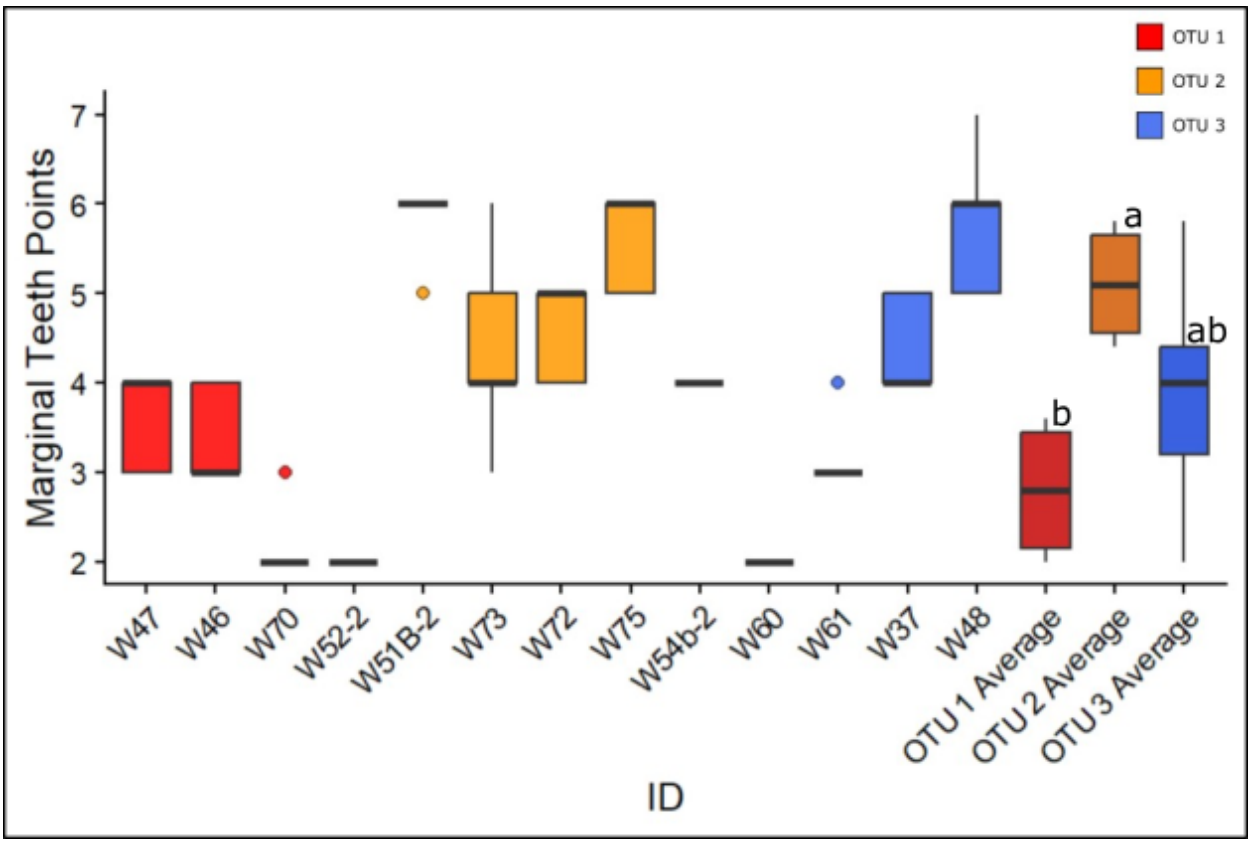

Figure 14: Box plots of marginal teeth points for OTU1, OTU2, and OTU3

Counts of marginal teeth points of five marginal teeth, from the anterior region of the radula, from 2 - 3 rows above the last row of inner lateral teeth (Fig. 2A). OTU # Averages (right side) are plots of all specimens' average counts of marginal tooth points grouped by OTU. Lower and upper box boundaries 25th and 75th percentile, respectively, line inside box median, lower and upper error lines furthest non-outlier point, colored dots outliers. Different letters above boxes indicate statistically significant differences among groups (Dunn's post hoc test following Kruskal–Wallis; $p < 0.05$). Groups sharing a letter are not significantly different. Inter-OTU Dunn test post hoc p-values are as follows: OTU1–OTU2: $P = .047$, OTU1-OTU3: $P = .83$, OTU2-OTU3: $P = .43$.

Egg Diameter

Egg diameter differed significantly among OTUs. OTU1 exhibited the largest mean egg diameter (86.5 µm), compared with OTU2 (77.1 µm) and OTU3 (74.6 µm) (Fig. 15). Tukey post hoc comparisons indicated strong significance between OTU1 and OTU2 and between OTU1 and OTU3 ($P < .001$), whereas OTU2 and OTU3 expressed less, but still significant differences, with highly overlapping ranges ($P = .05$) (Fig. 15).

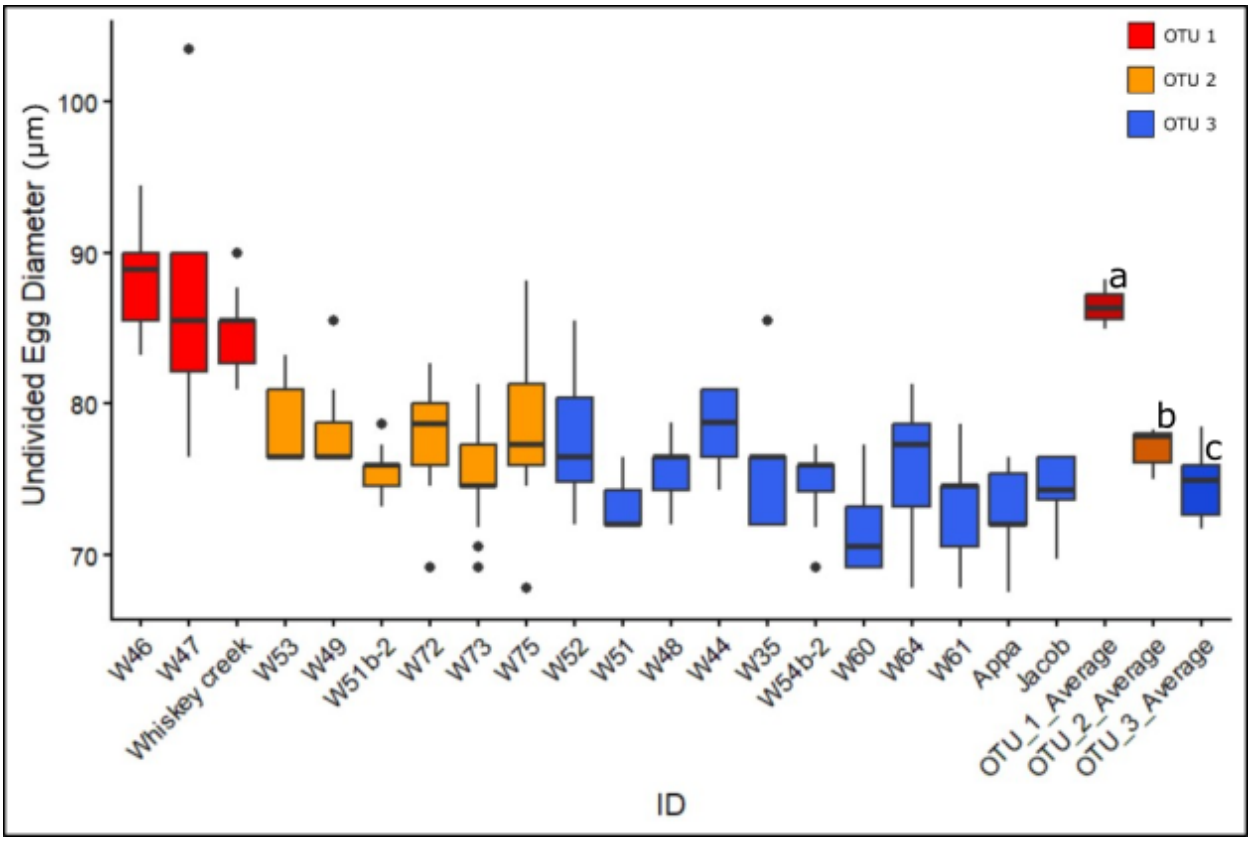

Figure 15: Box plots of egg diameters for OTU1, OTU2, and OTU3

Egg diameters (µm) reported for approximately 25 eggs per specimen. "OTU # Averages" (right side) are plots of all specimens' average marginal tooth point counts grouped by OTU. Lower and upper box boundaries 25th and 75th percentile, respectively, line inside box median, lower and upper error lines furthest non-outlier point, colored dots outliers. Individuals with W prefix were collected and barcoded for this investigation, all others come from work of Richard Emlet and Yvonne Moreira-Andrade. Different letters above boxes indicate statistically significant differences among groups (Tukey post hoc test following a one-way ANOVA; $p < 0.05$). Groups sharing a letter are not significantly different. Inter-OTU Tukey test post hoc p-values are as follows: OTU1–OTU2: $P < .001$, OTU1-OTU3: $P < .001$, OTU2-OTU3: $P = .05$.

Discussion

External Morphological Framework for OTU Identification

Morphological traits examined in this study—specifically caryophyllidial structure and minute spot aggregation—provide a complementary framework for distinguishing OTUs within the *Rostanga pulchra* cryptic species complex. While each character alone provides limited diagnostic resolution, their combined application enables consistent identification across the OTUs examined.

Caryophyllidial morphology differed significantly among OTUs (Fig. 3, Fig. 4, Fig. 6 & Table 3), consistent with the diagnostic value of caryophyllidia reported in other dorid nudibranchs (Muniaín et al., 2000; Innabi et al., 2023). Notably, within this complex, spicule position and relative height provided diagnostic value, whereas apical knob height was not significant. OTU1 displayed heavily inset spicules that lie beneath or level with the surrounding papula (Fig. 3, Fig. 4). In contrast, OTU2 regularly displayed tall spicules that extended far beyond the papula and were strongly outset or marginal (Fig. 3, Fig. 4). OTU3 exhibited an intermediate morphology, with moderately inset spicules that were commonly level with the surrounding papula (Fig. 3, Fig. 4).

Patterns of minute spots, a feature noted in the original description (MacFarland, 1905), and minute spot aggregation also differed among OTUs. OTU1 displayed a distinctive pattern consisting of large, conspicuous black spots formed by dense circular aggregations of minute pigment spots (Fig. 9). These aggregations were consistently observed across all specimens studied (n=5) as well as those observed previously (n=5) (Emlet, Unpublished), and provide a readily recognizable morphological feature for identifying OTU1. In contrast, minute spot patterns were far less informative for distinguishing OTU2 and OTU3. OTU3 exhibited

considerable variability, ranging from individuals lacking minute spots entirely to individuals with numerous aggregations (Fig. 9). OTU2 showed even more limited expression, with nearly all specimens lacking minute spots and a single individual displaying heavy spotting with indistinct aggregations (Fig. 9).

When considered together, these characters provide a practical morphological framework for identifying OTUs within the complex. The large black spot aggregations observed in OTU1 allow this lineage to be rapidly distinguished from the remaining OTUs. Once OTU1 is excluded, spicule position and proportional differences in spicule height allow OTU2 and OTU3 to be separated. In this way, minute spot aggregation functions as a coarse external character, while caryophyllidial morphology provides finer-scale diagnostic resolution.

Despite their diagnostic value, several limitations constrain the reliability of this morphological framework. For caryophyllidia, examination of ethanol-preserved specimens revealed the same overall trends in structure but with reduced statistical significance (Fig. 8), indicating that preservation may obscure subtle morphological differences detectable in live specimens. Moreover, in this study caryophyllidia were examined from the dorsal region anterior to the branchial plume. This region was selected based on preliminary observations that indicated morphological consistency. Variation in measured traits increased with distance from the medial line. Because of this gradient, supplemental sampling was conducted along the dorsal margin. Marginal caryophyllidia did not exhibit statistically significant differences among OTUs, and spicule position could not be reliably measured in these structures (Table 3). These results emphasize the importance of standardized sampling location when using caryophyllidial characters for species identification.

At present, this framework should be considered probabilistic, and needs refinement. Expanded sampling may clarify whether the heavy, indistinctly aggregated spotting observed in a single OTU2 specimen, as well as the minute spot aggregation observed in some OTU3 specimens, represents a consistent morphological variant could substantially strengthen this model. In addition, more precise measurements of spicule height and position may improve the resolution of caryophyllidial characters and strengthen their diagnostic utility. Overall, continued investigation of these traits, combined with broader sampling, will help determine the extent to which morphological variation can reliably resolve OTUs within this cryptic complex. Moreover, because caryophyllidial morphology is often described qualitatively but seldom quantified in species descriptions, the approach used here—systematically measuring spicule position and relative height—may offer a useful model for documenting subtle external variation in other cryptic nudibranch lineages.

Radular Morphological Framework for OTU Identification

Radular morphology has long been central to molluscan taxonomy and species descriptions and is frequently important in the delineation of cryptic species (Muniaín et al., 2000; Innabi et al., 2023; Matsuda et al., 2017; Innabi, 2023; Korshunova et al., 2019). In the present study, characters of the inner pleural tooth base provided the strongest diagnostic resolution among OTUs. Qualitative examination shifted focus from denticles and hooks to the lesser-described morphology of the tooth base, prompting two quantitative measurements: base angle and back nub length.

Base angle was diagnostic for OTU1, which exhibited angles three to four times wider than those observed in OTU2 and OTU3 (Fig. 11). Back nub length—the marginal facing

extension of the V-shaped base—also showed significant inter-OTU divergence (Table 4). OTU2 displayed the most distinctive morphology, with a back nub approximately twice the length observed in OTU1 and OTU3 (Fig. 12).

Together, base angle and back nub length provide a practical diagnostic framework for radular identification of OTUs. Angles exceeding 125° are most consistent with OTU1 (Fig. 11). Among specimens below this threshold, back nub lengths ≥8 μm are most consistent with OTU2, whereas shorter lengths align more closely with OTU3 (Fig. 12).

These thresholds should be interpreted probabilistically and will benefit from further examination with larger sample sizes (Table 4). Notably, although the base angles of OTU1 and OTU3 exhibited non-overlapping ranges, they did not produce a p-value below 0.05. This discrepancy may reflect the sensitivity of angular measurements to small deviations in specimen orientation during SEM imaging.

Although the ratio of inner lateral point lengths and marginal tooth point counts showed some statistical differences, their diagnostic utility is limited, though they may provide supplementary support. Both primarily reinforce identification of OTU1, which already possesses readily identifiable diagnostic features including the wide inner pleural tooth base angle and externally distinct large black spots. Because these teeth are not commonly described in species descriptions, further investigation of this divergence may provide limited taxonomic value.

Traditional radular characters commonly used in species descriptions—including half row counts, tooth length, and denticle counts—showed no statistical divergence among OTUs in this study (Table 4) and therefore lacked diagnostic value. The broad variation observed in half row counts likely reflects counting difficulty, as many specimens exhibited tightly spaced inner

laterals, damaged radulae, or obscuring organic material. In addition, counts were made from photographs rather than directly from the SEM, limiting maneuverability and measurement precision.

Further investigation of inner pleural tooth base morphology may reveal additional variation beyond the two measurements examined here. Expanded sampling and improved imaging precision will likely refine the diagnostic thresholds proposed in this study and clarify whether additional characters of the tooth base contribute to inter-OTU differentiation, further improving radular-based identification within this complex. More broadly, the diagnostic framework developed here may prove useful in the examination of other cryptic species complexes, where subtle variation in inner pleural tooth base morphology has historically received little attention.

Reproductive Traits and Life-History Divergence

Egg diameter is frequently reported in species descriptions and may reflect species-level divergence, although it is rarely used as a practical diagnostic character. Among the OTUs examined, OTU1 exhibited significantly larger eggs than OTU2 and OTU3 (Fig. 15). While this character does not contribute directly to the morphological framework used to identify OTUs, the observed difference suggests potential reproductive divergence among lineages within the complex. Increased egg size is generally interpreted as reflecting greater maternal investment and is often associated with reduced planktonic duration or adaptation to colder or more challenging environments (Todd 2001). If these life-history correlations hold within this complex, the enlarged eggs of OTU1 may indicate differences in developmental mode or dispersal potential relative to the other OTUs. Moreover, larval development has previously been

described for *Rostanga pulchra* (Anderson 1971), and reproductive differences have been documented between sister taxa *R. pulchra* and *R. byga* (Muniaín & Valdés 2000). Together, these previously published accounts and the egg size differences documented here highlight the potential for reproductive divergence within the complex and underscore the need for further investigation of life-history traits, which may ultimately contribute to future species-level descriptions.

Who is *Rostanga pulchra*?

Rostanga pulchra (MacFarland, 1905) was described prior to DNA barcoding, and thus its true OTU identity cannot be known. This section presents a hypothesis of OTU identity of the holotype, based on the confines of the original description and the metrics measured in this study. Based on inner pleural tooth morphology and minute spot aggregation, OTU3 most closely aligns with the nominal species. Notably this argument is a combination of the two frameworks mentioned above, as caryophyllidia are not described in adequate detail. Confirmation of this hypothesis requires examination of the holotype and additional sampling from Monterey Bay, CA, the type locality.

OTU1 can be excluded. MacFarland did not describe the large, conspicuous large black spots characteristic of OTU1, despite noting other variations in minute spot abundance and aggregation. Furthermore, his illustration of the inner pleural teeth (Fig. 16B) lacks the pronounced wide V-shaped base that distinguishes OTU1 (Figs. 9, 10; Table 4).

Minute spot patterns do not reliably distinguish OTU2 or OTU3 from the description, as both exhibit overlapping variation. Radular morphology provides stronger resolution. The only statistically significant radular difference between OTU2 and OTU3 is back nub length of the V-

shaped inner pleural tooth base (Table 4). MacFarland (1905 pg. 120) described the base as "short and broad" and illustrated it without a pronounced marginal extension (Fig. 16B), a condition consistent with OTU3, which exhibits a reduced back nub that can obscure the V-shape (Figs. 9, 11). In contrast, OTU2 possesses an elongated back nub that would likely have been evident in both description and illustration. Additionally, the wider angle between the inner pleural hook and medial-facing nub depicted by MacFarland more closely resembles OTU3 (Fig. 10). This angular relationship warrants further evaluation as a potential diagnostic character. Taken together, the available morphological evidence most strongly supports OTU3 as the best current hypothesis for the identity of *Rostanga pulchra*.

Importantly, the same newly characterized morphological traits that increase clarity in the true identity of *Rostanga pulchra* also clarify the distinctiveness of the remaining OTUs. In doing so, these characters establish a morphological framework that, together with genetic evidence, supports the formal description of two additional species, effectively resolving the cryptic species complex represented here. The transition from cryptic to diagnosable taxa carries implications well beyond the taxonomy of a single nudibranch lineage. Importantly, it refines biodiversity estimates and reveals patterns of species richness that would otherwise remain obscured (Bickford et al., 2006). Establishing consistent morphological diagnoses also enables the replication of this framework in related taxa, converting additional cryptic relations into new biodiversity, facilitating further systematic progress (Matsuda and Gosliner, 2017). In turn, improved species resolution strengthens conservation planning, ensures that distinct lineages are recognized and managed appropriately, and provides a clearer foundation for interpreting ecological specialization and evolutionary diversification within clades (Bickford et al., 2006; Prieto-Baños, 2025).

By establishing diagnostic morphological characters within the *Rostanga pulchra* complex, this study therefore not only advances the identification of the nominal species but also lays the groundwork for formal species descriptions that contribute to a more accurate understanding of dorid nudibranch biodiversity and its broader ecological and evolutionary significance.

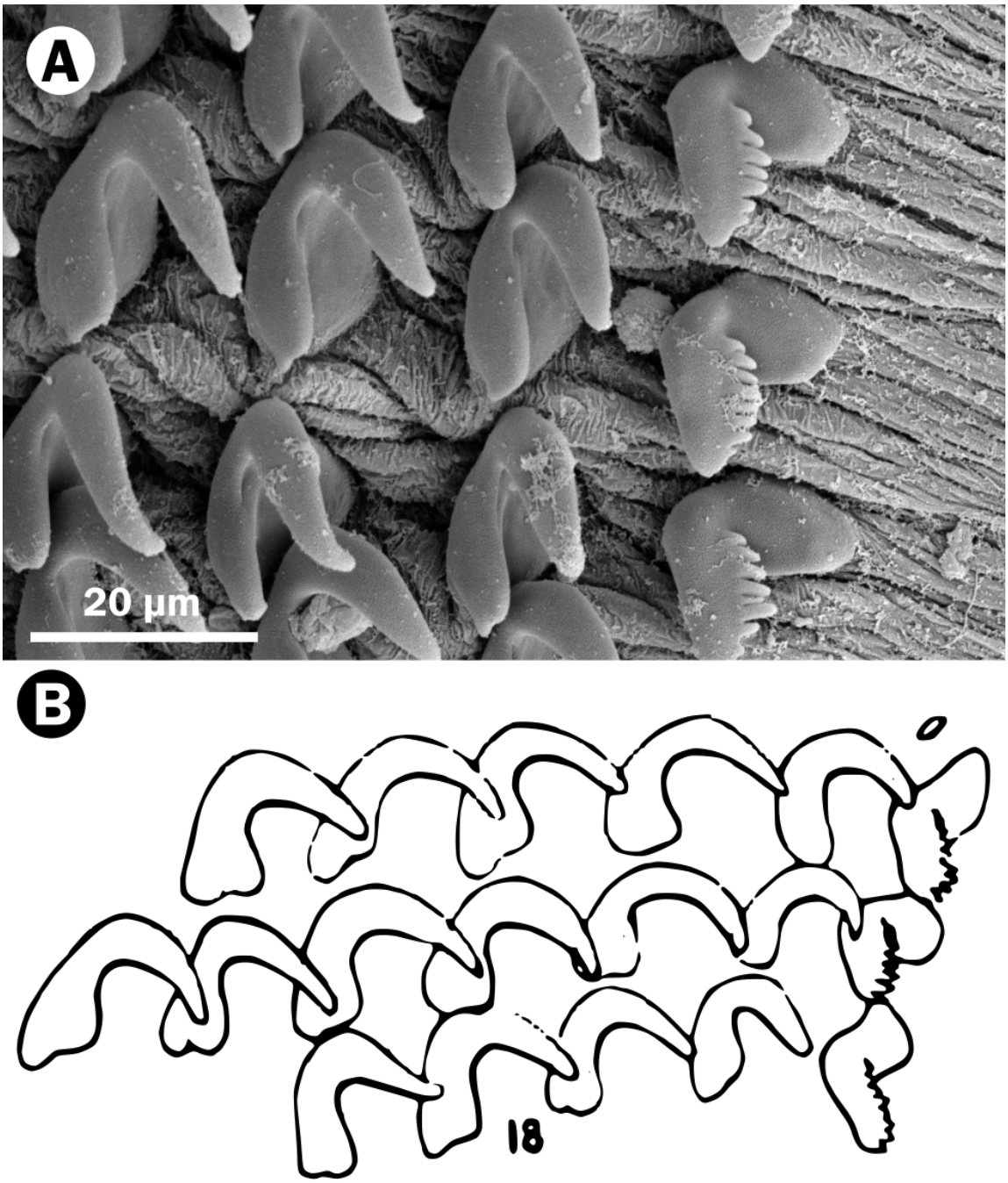

Figure 16: Comparison of W60 (OTU3) inner pleural teeth and diagram from original description

A) SEM photo of W60, an individual belonging to OTU3 taken at a similar angle as B) “Diagram 18” from the original description of *Rostanga pulchra,* depicting inner pleural and inner lateral teeth (MacFarland 1905).

Conclusion

Taxonomic research provides the framework through which biological diversity is described, compared, and understood. This thesis contributes to that framework by establishing morphological parameters for distinguishing members of the *Rostanga pulchra* cryptic species complex and by integrating those observations with molecular evidence.

The analyses presented here demonstrate that fine-scale morphological characters provide reliable criteria for distinguishing lineages within the *Rostanga pulchra* complex. External morphology revealed informative variation in caryophyllidial structure and pigmentation patterns, while radular morphology provided an equally robust diagnostic framework. In particular, previously underutilized characters of the inner pleural tooth base—base angle and back nub length—proved effective for distinguishing OTUs. Together, these traits establish a practical morphological framework for identifying members of the complex. The approaches used here to quantify subtle external and radular characters may also provide a useful model for investigating morphological variation in other cryptic species complexes. This highlights the continued value of careful morphological observation—reminiscent of the "golden age" of descriptive biology—even in the era of modern molecular tools. At the same time, the relatively small proportion of traits that proved consistently diagnostic illustrates the limitations of morphology alone and underscores the strength of DNA barcoding as a complementary approach.

Egg diameter provided additional biological context, with OTU1 exhibiting significantly larger eggs than OTU2 and OTU3, suggesting potential divergence in reproductive strategy or developmental mode. Although not directly diagnostic, such life-history differences highlight

avenues for future research that may further clarify ecological and evolutionary divergence within the group.

Comparison with the original description suggests that OTU3 most closely corresponds to the nominal species *Rostanga pulchra*, while OTU1 and OTU2 likely represent undescribed species. By revealing diagnostic morphological traits within a 100-year-old cryptic complex, this study contributes to a more accurate understanding of dorid nudibranch biodiversity, carrying implications into related fields of ecology, conservation, and evolution. As pressures on marine ecosystems intensify and species distributions shift, the ability to accurately account for biodiversity becomes increasingly critical. Taxonomic work such as this not only clarifies evolutionary relationships but also ensures that distinct lineages are recognized before ecological change obscures or eliminates them. In this way, careful documentation of species diversity remains a foundational step toward understanding and conserving the richness of life in the oceans.

Biography

Anderson, E., The Association of the Nudibranch *Rostanga pulchra* MacFarland 1905 with the Sponges *Ophlitaspongia Pennata, Esperiopsis Originalis,* and *Plocamia karykina. UCSC*

Bickford, D., Lohman, D., Sodhi, N., Ng, P., Meier, R., Winker, K., Ingram, K., Das, I., Cryptic species as a window on diversity and conservation. *Trends in ecology & evolution 22.3* (2007): 148-155. https://doi.org/10.1016/j.tree.2006.11.004

Bloom, S., Morphological correlations between dorid nudibranch predators and sponge prey. *The Veliger* 1976; 18: 289-301

Churchill, C., Valdes, A., Foighill, D., Molecular and morphological systematics of Neustonic Nudibranchs (mollusca : Gastropoda : Glaucidae : Glaucus), with descriptions of three new cryptic species." *Invertebrate Systematics*, vol. 28, no. 2, 2014, p. 174, https://doi.org/10.1071/is13038.

Dean, Lewis J., and Michèle R. Prinsep. "The chemistry and chemical ecology of nudibranchs." *Natural product reports* 34, no. 12 (2017): 1359-1390.

Faucci, A., Toonen, R., Hadfield, M., Host shift and speciation in a coral-feeding nudibranch. *Proceedings. Biological sciences* vol. 274,1606 (2007): 111-9. doi:10.1098/rspb.2006.3685

Fernández-Vilert, R., Arnedo, M., Salvador, X., Valdés, Á., Schrödl, M., Moles, J., Shining disco: shedding light into the systematics of the family Discodorididae (Gastropoda: Nudibranchia), *Zoological Journal of the Linnean Society,* Volume 203, Issue 1, January 2025, zlae170, https://doi.org/10.1093/zoolinnean/zlae170

Fišer, C., Robinson, C., Malard, F., Cryptic Species as a Window into the Paradigm Shift of the Species Concept. *Molecular Ecology,* vol. 27, no. 3, Feb. 2018, pp. 613–35. DOI.org (Crossref), https://doi.org/10.1111/mec.14486.

Foale, S.J., Willan, R.C. Scanning and transmission electron microscope study of specialized mantle structures in dorid nudibranchs (Gastropoda: Opisthobranchia: Anthobranchia). *Mar. Biol.* 95, 547–557 (1987). https://doi.org/10.1007/BF00393098

Folmer, O., Black, M., Hoeh, W., Lutz, R., & Vrijenhoek, R. 1994. DNA primers for Amplification of mitochondrial cytochrome c oxidase subunit I from diverse Metazoan invertebrates. *Mol. Mar. Biol.* Biotech. 3: 294–299.

Fox, Sof (2024). One Nudibranch One Sponge? Using Genetic Barcoding to Analyze the *Rostanga pulchra* Species Complex and Prey Differentiation. *Undergraduate Research, University of Oregon.*

Gannon, E., The Art of a Slugslayer: An Exploration of the Process of Extracting Radulae from *Lehmannia valentiana* for the Purpose of Viewing in the Scanning Electron Microscope (2023). *Mahurin Honors College Capstone Experience/Thesis Projects.* Paper 1018. https://digitalcommons.wku.edu/stu_hon_theses/1018'

Garovoy, J., Valdés, Á., Gosliner, T., Phylogeny of the Genus *Rostanga* (Nudibranchia), with Descriptions of Three New Species from South Africa, *Journal of Molluscan Studies,* Volume 67, Issue 2, 2001, Pages 131–144, https://doi.org/10.1093/mollus/67.2.131,

Geiger, D., Marshall, B., Ponder, W., Sasaki, T., Techniques for Collecting, Handling, Preparing, Storing and Examining Small Molluscan Specimens. *Molluscan Research*, vol. 27, nos. 1–50, DOI:10.11646/mr.27.1.1

Goddard, J. The Opisthobranchs of Cape Arago, Oregon, With Notes on Their Natural History and a Summary of Benthic Opisthobranchs Known from Oregon. *Thesis (M.S.)--University of Oregon, 1983.*

Gosliner T.M. 1994. Gastropoda: Opisthobranchia. In: Harrison FW, Kohn AJ, editors. *Microscopic anatomy of invertebrates. Vol. 5: Mollusca I.* New York (NY): Wiley-Liss. p. 253–355.

Hadfield, M.G., Switzer-Dunlap, M. (1984) Opisthobranchs. In: Tompa, A.S., Verdonk, N.H. & van den Biggelaar, J.A.M. (Eds), *The Mollusca, Reproduction.* Academic Press, London, pp. 209–350.

Innabi, J., Stout, C., Valdés, Á. Seven new 'cryptic' species of Discodorididae (Mollusca, Gastropoda, Nudibranchia) from New Caledonia. Zookeys. 2023 Mar 7;1152:45-95. Doi:10.3897/zookeys.1152.98258. PMID: 37214742; PMCID: PMC10194415.

Jörger, K.M., Schrödl, M. How to describe a cryptic species? Practical challenges of molecular taxonomy. *Front Zool* 10, 59 (2013). https://doi.org/10.1186/1742-9994-10-59

Jensen, K., Morphological adaptations and plasticity of radular teeth of the Sacoglossa (=Ascoglossa) (Mollusca: Opisthobranchia) in relation to their food plants, *Biological Journal of the Linnean Society*, Volume 48, Issue 2, February 1993, Pages 135–155, https://doi.org/10.1111/j.1095-8312.1993.tb00883.x

Korshunova, T., Martynov, A., Bakken, T., Picton, B., External Diversity Is Restrained by Internal Conservatism: New Nudibranch Mollusc Contributes to the Cryptic Species Problem. *Zoologica Scripta*, vol. 46, no. 6, Nov. 2017, pp. 683–92. DOI.org (Crossref), https://doi.org/10.1111/zsc.12253.

Korshunova, T., Driessen, F., Picton, B., Martynov, A., The multilevel organismal diversity approach deciphers difficult to distinguish nudibranch species complex. *Scientific Reports*, vol. 11, no. 1, 15 Sept. 2021, https://doi.org/10.1038/s41598-021-94863-5.

Lindsay, T., Kelly, J., Chichvarkhin, A., Craig, S., Kajihara, H., Mackie, J., & Valdés, Á. (2016). Changing spots: pseudocryptic speciation in the North Pacific dorid nudibranch Diaulula sandiegensis (Cooper, 1863)(Gastropoda: Heterobranchia). *Journal of Molluscan Studies*, *82*(4), 564-574.

MacFarland, F. Opisthobranchiate Mollusca from Monterey Bay, California, and Vicinity. *Bulletin of the Bureau of Fisheries,* 1905.

Matsuda, S., Gosliner, T. Molecular phylogeny of Glossodoris (Ehrenberg, 1831) nudibranchs and related genera reveals cryptic and pseudocryptic species complexes. *Cladistics*. 2018 Feb;34(1):41-56. doi:10.1111/cla.12194. Epub 2017 Feb 28. PMID: 34641635.

Moreiria-Andrade, Y. (2024). Looking for Ecological Differences Among 3 Clades of *Rostanga pulchra* - Habitat, Sponge Prey, Body size and Egg size. *Undergraduate Research, University of Oregon*

Muniaín, C., and Valdés A., *Rostanga byga* Er. Marcus, 1958 from Argentina: redescription and comparison to *Rostanga pulchra* MacFarland, 1905 (Mollusca, Nudibranchia, Doridina). Vol. 52. No. 1. *California Academy of Sciences,* 2000.

Neuhaus, J. Systematic revision of the genus *Jorunna* (Nudibranchia: Discodorididae) in Europe with a focus on the *J. tomentosa* species complex. *Master's Thesis* (2020): 122.

Penney, B. K. (2006). Morphology and biological roles of spicule networks in *Cadlina luteomarginata* (Nudibranchia, Doridina). *Invertebrate Biology,* 125, 222–232. https://doi.org/10.1016/j.jcz.2025.06.001

Prieto-Baños, Silvia, and Kara KS Layton. "Tracing the evolution of key traits in dorid nudibranchs." *Plos one* 20, no. 4 (2025): e0317704.

Reid, D., Mak, Y., Indirect evidence for ecophenotypic plasticity in radular dentition of *Littoraria* species (Gastropoda: Littorinidae), *Journal of Molluscan Studies*, Volume 65, Issue 3, August 1999, Pages 355–370, https://doi.org/10.1093/mollus/65.3.355

Schrödel, M., Grau, J., 2006. Nudibranchia from the remote southern Chilean Guamblin and Ipún islands (Chonos Archipelago, 44-45° S), with re-description of *Rostanga pulchra* MacFarland, 1905 DOI: 10.4067/S0716-078X2006000100001

Schroedl, Michael. (2003). Sea slugs of southern South America: systematics, biogeography and biology of Chilean and Magellanic Nudipleura (Mollusca-Opisthobranchia).
Steinke, D., Prosser, S. W. J., & Hebert, P. D. N. (2016). DNA barcoding of marine metazoans. *Methods in Molecular Biology*, 1452, 155–168. https://doi.org/10.1007/978 1-4939-3774-5_10

Stephen, A., Bloom, C., Radular Variation in Two Species of Sponge-rasping Dorid Nudibranchs, *Journal of Molluscan Studies,* Volume 43, Issue 3, December 1977, Pages 296–300, https://doi.org/10.1093/oxfordjournals.mollus.a065384

Tisdale, Jackson (2024). Radular Characteristics of Rostanga pulchra. *Undergraduate Research, University of Oregon.*

Todd, Christopher D., J. Walter, and Jon Daviee. "Some perspectives on the biology and ecology of nudibranch molluscs: generalisations and variations on the theme that prove the rule." *Bollettino Malacologico* 37 (2001): 105-120.

Trickey, J. S., Vanner, J.,Wilson, N. G. (2013). Reproductive variance in planar spawning Chromodoris species (Mollusca: Nudibranchia). *Molluscan Research*, 33(4), 265–271. https://doi.org/10.1080/13235818.2013.801394

Valdés, Á., Gosliner, T., Systematics and phylogeny of the caryophyllidia-bearing dorids (Mollusca, Nudibranchia), with descriptions of a new genus and four new species from Indo-Pacific deep waters, *Zoological Journal of the Linnean Society,* Volume 133, Issue 2, 2001, Pages 103-198, ISSN 0024-4082, https://doi.org/10.1006/zjls.2000.0261.

Valdés, Á., Phylogeography and phyloecology of dorid nudibranchs (Mollusca, Gastropoda), *Biological Journal of the Linnean Society,* Volume 83, Issue 4, December 2004, Pages 551–559, https://doi.org/10.1111/j.1095-8312.2004.00413.x